ISTANBUL TECHNICAL UNIVERSITY ★ GRADUATE SCHOOL OF SCIENCE ENGINEERING AND TECHNOLOGY

CONSTRUCTION OF A FUNCTIONAL BIODEGRADABLE BONE TISSUE ENGINEERING SCAFFOLD FOR ENHANCED BIOMINERALIZATION

M.Sc. THESIS

İnas ÖZCAN

Department of Molecular Biology-Genetics and Biotechnology

Molecular Biology-Genetics and Biotechnology Programme

DECEMBER 2016

ISTANBUL TECHNICAL UNIVERSITY ★ GRADUATE SCHOOL OF SCIENCE ENGINEERING AND TECHNOLOGY

CONSTRUCTION OF A FUNCTIONAL BIODEGRADABLE BONE TISSUE ENGINEERING SCAFFOLD FOR ENHANCED BIOMINERALIZATION

M.Sc. THESIS

İnas Özcan
(521131127)

Department of Molecular Biology-Genetics and Biotechnology

Molecular Biology-Genetics and Biotechnology Programme

Thesis Advisor: Assoc. Prof. Dr. Fatma Neşe KÖK

DECEMBER 2016

İSTANBUL TEKNİK ÜNİVERSİTESİ ★ FEN BİLİMLERİ ENSTİTÜSÜ

BİYOMİNERALİZASYONU TETİKLEYEN, FONKSİYONEL VE BİYOBOZUNUR BİR KEMİK DOKU MÜHENDİSLİĞİ İSKELESİ YAPIMI

YÜKSEK LİSANS TEZİ

İnas Özcan
(521131127)

Moleküler Biyoloji-Genetik ve Biyoteknoloji Anabilim Dalı

Moleküler Biyoloji-Genetik ve Biyoteknoloji Programı

Tez Danışmanı: Doç. Dr. Fatma Neşe KÖK

ARALIK 2016

İnas Özcan, a MSc student of ITU Graduate School of Science, Engineering and Technology student ID 521131127, succesfully defended the thesis entitled "CONSTRUCTION OF A FUNCTIONAL BIODEGRADABLE BONE TISSUE ENGINEERING SCAFFOLD FOR ENHANCED BIOMINERALIZATION", which she prepared after fulfilling the requirements specified in the associated legislations, before the jury whose signatures are below.

Thesis Advisor :	**Assoc Prof Dr Fatma Neşe KÖK** Istanbul Technical University	.....
Jury Members :	**Prof. Dr. Zeynep Petek ÇAKAR** Istanbul Technical University	.....
	Prof.Dr. Sedef TUNCA GEDİK Gebze Technical University	.....

Date of Submission : 25 November 2016
Date of Defense : 20 December 2016

To my family,

FOREWORD

Firstly, I would like to special thank my sincere gratitude to my supervisor Assoc. Prof. Dr. Fatma Neşe KÖK for her guidance, encouragement, understanding and patience during my master programme. She has a wonderful friendship and cheerfulness that I appreciate as always.

I would also like to thank Assist Prof Sakip Önder, Sevgin Türkeli, Dr Barbaros Akkurt for their time and support for scanning electron microscope images and fourier transform infrared spectra of scaffolds and Prof Dr Kürşat Kazmanlı and Prof Dr Ahmet Gül for allowing us to use equipments in their laboratories.

Additionally, I want to special thanks to my lab-mates Burak Ağbaba for his support, and collaborate with my thesis and Ayşe Buse Özdabak, Beren Şen, Abdulhalim Kılıç for their helps, supports and great friendships during studying with wonderful days in our laboratories. In addition, I would like to thank Gökçe Bekaroğlu and Ayşe Ceren Çalıkoğlu for teaching me about cell culture experiments and supports with great friendships.

I have a lot of special friends that I never let them leave from my life. We have excellent relationships that we cannot break each other and keep them as long as we can. A huge bunch of loves goes to these people for being in my life.

Finally, I would also to thank Selva Özcan, my mother, Sabahattin Özcan, my father, Yunus and Enes Özcan my brothers for being in my life with their great supports, and faiths in me to make me more courageous. They always with me and do anything for me to actualize my wishes in my life.

November 2016 İnas ÖZCAN

TABLE OF CONTENTS

Page

ABBREVIATIONS

3D	**:** Three-dimensional
TGF-β1	**:** Transforming Growth Factor Beta 1
IGF	**:** Insulin-like Growth Factor
VEGF	**:** Vascular Endothelial Growth Factor
PGA	**:** Poly (glycolide)
PLA	**:** Poly (lactide)
PCL	**:** Poly (caprolactone)
PE	**:** Poly (ethylene)
PMMA	**:** Poly (methyl methacrylate)
TCP	**:** Tricalcium Phosphate
DCP	**:** Dicalcium Phosphate
HAp	**:** Hydroxyapatite
ACP	**:** Amorphous Calcium Phosphate
Leu	**:** Leucine
Glu	**:** Glutamic Acid
Pro	**:** Proline
Arg	**:** Arginine
Val	**:** Valine
Cys	**:** Cysteine
Asn	**:** Asparagine
Gly	**:** Glycine
Ala	**:** Alanine
Ser	**:** Serine
Ca	**:** Calcium
P	**:** Phosphorus
Mg	**:** Magnesium
Na	**:** Sodium
Cl	**:** Chloride
Na_2CO_3	**:** Sodium Carbonate
OH^-	**:** Hydroxyl
CO_3^{2-}	**:** Carbonate
CO_2	**:** Carbon Dioxide
PO_4^{3-}	**:** Phosphate
CH_2	**:** Methylene
CH_3	**:** Methyl group
mSBF	**:** Modified Simulated Body Fluid
COOH	**:** Carboxylic Acid
PLLA	**:** Poly (L-Lactide acid)
SF	**:** Silk Fibroin
CAD	**:** Computer-Aided Design
UV	**:** Ultraviolet
BMP-2	**:** Bone Morphogenetic Protein-2
FDA	**:** Food and Drug Administration

RGD : Arginine-Glycine-Aspartic Acid
BSP : Bone Sialoprotein
OPN : Osteopontin
RADA-16 : Arginine-Alanine-Aspatic Acid-Alanine-16
CBM : Collagen Binding Motif
NH_2 : Amine
HFIP : Hexafluoroisopropanol
EDC : 1-ethyl-3-(3-dimethylaminopropyl) carbodiimide
NHS : N-hydroxysuccinimide
MES : 2-(N-morpholino) ethanesulfonic acid
PBS : Phosphate Buffered Saline
SEM : Scanning Electron Microscopy
EDS : Energy-dispersive X-ray spectroscopy
FTIR : Fourier Transform Infrared Spectroscopy
hFOB : Human Fetal Osteoblast
DMEM : Dulbecco's Modified Eagle Medium
MeOH : Methanol

SYMBOLS

%	**:** Per cent
℃	**:** Degree Centigrade
kDa	**:** Kilodalton
min	**:** Minute
L	**:** Litre
M	**:** Molar
N	**:** Normal
rpm	**:** Revolutions per Minute
mL	**:** Mililitre
g	**:** Gram
w/v %	**:** Weight/Volume per cent
w/w %	**:** Weight/Weight per cent
pH	**:** Power of Hydrogen
μg/mL	**:** Microgram per Volume Solution Concentration
U/mL	**:** Units per Volume Solution Concentration
g/L	**:** Grams per Volume Solution Concentration
μL	**:** Microliter
nm	**:** Nanometer
cm^{-1}	**:** Wavenumber
%T	**:** % Transmittance

LIST OF TABLES

Page

LIST OF FIGURES

Page

CONSTRUCTION OF A FUNCTIONAL BIODEGRADABLE BONE TISSUE ENGINEERING SCAFFOLDS FOR ENHANCED BIOMINERALIZATION

SUMMARY

In case of accidents, injuries or diseases, a various tissue deformations may occur. Tissue regenerations can take a long time and sometimes recovery is not possible completely. The metals, polymers and ceramics are widely used in biomedical field to assist the body to address these problems. Tissue engineering aims to produce tissues by mimicing natural structures with using natural and synthetic polymeric scaffolds.

This study aims to obtain composite scaffolds for bone tissue regeneration using silk fibroin and poly(l-lactide) as natural and synthetic polymers. These scaffolds were produced by freeze drying method and insulation cover was used to observe the effect of freezing conditions on properties of scaffolds. After lyophilization process, the scaffolds were treated with methanol to induce beta sheet regions from random coil structures in silk fibroin protein. To induce biomineralization, various peptides can be used. In this study, OSN peptide, which is obtained from osteocalcin protein, was used to promote hydroxyapatite (HAp) crystallization. The scaffolds were characterized with water uptake, biodegradation, biomineralization and cell proliferation tests.

The water uptake capacities of scaffolds were found to be higher than 400% for both SF:PLLA (1:3 w/w) and SF:PLLA (3:1 w/w) scaffolds. The samples with high silk fibroin ratio had higher water uptake capacity (almost two fold) compared to other ones. The degradation analysis was carried out for two month. The protease XIV enyzme (0.1U/mL) was used to see its effect on fibroin degradation. After two months, the remaining weight of SF:PLLA (1:3 w/w) and SF:PLLA (3:1 w/w) scaffolds were higher than 50% with and without enzyme. As expected, sample with high SF showed more degradation in the presence of protease enzyme.

The effect of methanol treatment on formation of beta sheet structures from random coils were investigated with FTIR analysis by observing shifted peaks at amide I and amide II regions for SF:PLLA (1:3 w/w) and only amide I region for SF:PLLA (3:1 w/w) scaffolds. After methanol treatment, the insoluble structures were obtained with increasing beta sheet formations in fibroin proteins and used for further analysis.

The mineralization process was followed for a month and weight changes of scaffolds were reported. Two events simultaneously occur in solution: The formation of apatite crystals and degradation of polymers and weight of scaffolds was affected from both. The scaffolds that were incubated in 3xmSBF solution showed weight loss at the end of a month. On the other hand, the scaffolds incubated in 1xmSBF showed weight gains after a month. The effect of OSN peptides could not be clearly observed from weight change data.

The SEM images were taken and the atomic ratios of Ca/P were determined by EDS after 2, 3 and 4^{th} weeks of mineralization process. According to the SEM images, mineral formations can be observed after 2^{nd} week in scaffolds with and without peptides in 1xmSBF and 3xmSBF solutions. The Ca/P ratios were calculated in scaffolds incubated in 1xmSBF solution. The calcification appeared because of the more calcium accumulation after 3^{rd} and 4^{th} weeks of mineralization. The Ca/P ratios of SF:PLLA (3:1 w/w) scaffolds with peptides after 4^{th} week of mineralization and SF:PLLA (1:3 w/w) scaffolds with peptides after 2^{nd} week of mineralization were found to be closer to the stoichiometric value of HAp (1.67).

The FTIR spectra were obtained for both scaffolds without peptides incubated in 3xmSBF solution. The presence of characteristic groups of PLLA made diffucult to distinguish the groups of HAp crystals. The few absorption peaks shifted because of the apatite growth on polymer surfaces. The CO_3^{2-}, PO_4^{3-}, type A and B carbonate (CO_3HAp) and OH^- groups that belongs to HAp crystals were obtained on scaffolds especially after 1^{th} week of mineralization according to the FTIR spectra.

To investigate the proliferation of human osteoblast cells (hFOB) on composite scaffolds, MTS analysis was applied at 1, 4 and 7 day. The SF:PLLA (3:1 w/w) scaffolds showed higher cell numbers than SF:PLLA (1:3 w/w) scaffolds. Additionally, the SF:PLLA (1:3 w/w) with peptides had more hFOB cells on polymer surfaces than without peptides scaffolds. On the other hand, the SF:PLLA (3:1 w/w) scaffolds with peptides showed less cell proliferation than without peptides forms.

In conclusion, the composite scaffolds with two different concentrations were produced by lyophilization process to mimic bone tissue structures and a peptide to direct the mineralization process was added for further improvement. The biodegradability of the scaffolds seemed to be appropriate for bone tissue engineering. Peptide addition affected the mineralization and cell proliferation behavior of the scaffolds but not always in positive manner. For future prospects, the labeled-peptides can be used to obtain the distribution of peptides on the surfaces of polymers. HPLC analysis can be applied to optimize the concentration of immobilized peptides. In addition, the *von Kossa* staining can be used to observe calcium deposition. In sum, a more comprehensive study is needed to understand and optimize the effect of peptides on the scaffolds surface.

BİYOMİNERALİZASYONU TETİKLEYEN, FONKSİYONEL VE BİYOBOZUNUR BİR KEMİK DOKU MÜHENDİSLİĞİ İSKELESİ YAPIMI

ÖZET

Yaşanılan birtakım kazalar, yaralanmalar ya da hastalıklar, insan vücudunda çeşitli doku kayıplarına, deformasyonlara sebep olabilmektedir. Bu doku kayıplarının rejenerasyonu uzun zaman alabilmekte ve eski yapının oluşmasında zorluklar ortaya çıkabilmektedir. Bu problemlerin çözümü için çeşitli biyomalzemeler kullanılmaktadır. Her geçen yıl gelişen ve çeşitlenen biyomedikal çalışmalarında ilk zamanlarda metal, alaşım protezler, plaklar, vidalar ve seramik malzemeler kullanılırken son yıllarda polimerler daha sık tercih edilmektedir. Bunlara ek olarak canlı hücrelerin ve çeşitli doğal ve sentetik polimerlerin birlikte kullanımını içeren doku mühendisliği son zamanlarda araştırmacıların odak noktası haline gelmiştir.

Doku rejenerasyonuna yardım ve destek için sıkça kullanılan metal, alaşım vb. malzemeler ile doku onarımı daha uzun sürede gerçekleşmekte ve hasta için ikinci bir operasyonu gerektirmektedir. Buna kıyasla çeşitli kaynaklardan elde edilen polimer malzemeler, doğal doku yapısı ile daha fazla benzer özellik taşıdığı ve kolayca modifiye edilebildiği için daha sık kullanılmaya başlamıştır. Polimerler; doğal kaynaklardan elde edilen (kitosan, jelatin, fibroin vb.) ve çeşitli kimyasal sentez yöntemleri ile üretilen sentetik polimerler olarak iki sınıftan oluşmaktadır. Çeşitli çalışmalar, yeni dokunun oluşum sürecinde implante edilen polimerik malzemelerin biyobozunurluk, biyouyumluluk, toksik olmama gibi özellikleri ile rejenerasyonunu daha kısa sürede geliştirdiğini göstermektedir.

Doku mühendisliğinde polimerler çeşitli formlarda kullanılmaktadır. Nanofiber, sünger, mikroküre, film gibi birçok formlar doku rejenerasyonu için denenen bazı formlardır. Sert doku mühendisliğinde daha sık kullanılan polimerik sünger yapılarının, istenen özellikleri kazandırma amacıyla mikroküre, nanofiber gibi diğer formlar ile kompozisyonu yapılabilmektedir. Doku çeşidine göre değişen özellikleri kazandırma amacıyla, farklı polimerler farklı konsantrasyonlarda bir araya getirilerek çeşitli kompozit yapılar ve doğal yapıya benzer mikroçevreler oluşturulmaktadır.

Çeşitli kırıklar, deformasyonlar sonucu zarar gören kemik dokusu uzun sürede rejenere olmaktadır. Kemik yapısında bulunan osteopontin, osteokalsin gibi proteinler ile organik ve anorganik kısımların sentezi, doku onarımında önemli bir süreçtir. Kemiğin majör bileşeni olan anorganik kısımdaki hidroksiapatit yapısının oluşumu, kemik rejenerasyonundaki en önemli süreçlerden biridir. Bu sebeple kemik doku mühendisliğinde sadece hücre tutunması, proliferasyonu ve göçünün sağlanması değil, hidroksiapatit yapısının kemiğe benzer şekilde oluşması için uygun doku mühendisliği iskelelerinin hazırlanması gereklidir ve ancak bu şekilde doku onarım süreci hızlandırılabilmektedir.

Kemik doku mühendisliğinde oluşturulan polimerik doku iskelelerin birtakım spesifik özellikleri taşıması gerekmektedir. Biyouyumlu, toksik olmama, kontrol edilebilir bozunma süreci, gözenekli yapı gibi özellikleri ile birlikte osteokondüktif, osteoindüktif ve osteojenik yapıda olmaları gerekmektedir. İstenen bu özelliklerdeki doku iskeleleri için genellikle birden fazla polimer ile kompozit yapılması ya da yüzey modifikasyonları gibi teknikler ile polimerlerin özelliklerinin geliştirilmesi gerekmektedir.

Doku mühendisliğinde çeşitli peptit dizileri fiziksel ve kimyasal yollar ile polimer doku iskelelerinin yüzeylerine immobilize edilmekte ve bu şekilde hücre tutunması ve proliferasyonlarını arttırmak mümkün olmaktadır. Bunların yanında kemik doku mühendisliğinde hidroksiapatite bağlanabilen ya da bu tür mineralleşmeyi tetikleyebilen bazı peptit dizileri de kullanılabilmektedir. Bu peptit dizilerinin immobilizasyonu ile biyomineralizasyon süreci hızlandırılmakta, minerallerin kemiktekine benzer şekilde oluşması sağlanabilmekte ve osteoblast hücrelerin tutunması arttırılmaktadır. Böylece hidroksiapatit bileşenin hızlı oluşumu sonucu kemik doku rejenerasyonu daha kısa sürede gerçekleşmektedir.

Kemiğin yapısında bulunan en önemli proteinlerden biri olan osteokalsin proteini, 44 amino asit dizisine sahiptir. Bir çalışmada osteokalsin protein dizisinden hidroksiapatit yapılarına bağlanabilme özelliğine sahip 13 amino asitlik bir peptit dizisi kullanılmıştır. Bu peptit dizisinin, OSC ve OSN olarak sırasıyla serbest uç (hidroksil) ve amin grubu ile biten formları çalışılmıştır. OSN peptit dizisinin biyomineralizasyonu kısa sürede arttırdığı bilinmektedir. Bu peptit dizisi ile ilgili çalışmalar sadece paslanmaz çelik yüzeyleri ile sınırlı olduğundan polimer yüzeylerde davranışı bu tez çalışması ile araştırılmıştır.

Islak çekme, tuz giderme, faz ayrımı, gaz köpüklendirme ve dondurarak kurutma gibi teknikler üç boyutlu doku iskeleleri üretiminde kullanılmaktadır. Doku iskelesinin gözeneklilik özelliğini şekillendiren en önemli etkenlerden biri de üretim tekniğidir. Bu üretim tekniklerinde birtakım koşullar değiştirilerek değişik gözeneklilik ve mekanik özellikler elde edilebilmektedir.

Bu çalışmada doğal ipek fibroin protein (SF) ve sentetik poli(l-laktik asit) (PLLA) polimeri ile 3% w/v konsantrasyonlarda kompozit doku iskeleleri oluşturulmuştur. Liyofilizasyon yöntemi ile yalıtım malzemesi kullanılarak gözenekli doku iskeleleri oluşturulmuştur. Yalıtım malzemesinin gözenekli yapı oluşumundaki etkisi incelenmiştir. Liyofilizasyon ardından metanol ile muamele edilerek fibroin yapısındaki düzensiz kıvrımların (random coil) beta-tabakalı konfigürasyonlara dönüşümü sağlanmıştır. HAp oluşumunu hızlandırmak için osteokalsin proteininden elde edilen OSN peptit dizileri kullanılmıştır. Ardından doku iskeleleri, su alma kapasiteleri, biyobozunurluk, biyomineralizasyon ve hücre çoğalması testleri ile incelenmiştir.

SF:PLLA (1:3 w/w) ve SF:PLLA (3:1 w/w) doku iskelelerinin su alma kapasitelerinin %400'den fazla olduğu tespit edilmiştir. Yüksek konsantrasyonda fibroin içeren doku iskelelerinin diğer doku iskelelerine göre daha yüksek su tutma kapasiteleri olduğu (neredeyse iki katı kadar) görülmüştür. Bozunurluk testi, iki ay süresince yapılmıştır. Proteaz XIV enziminin (0.1U/mL) fibroin proteininin bozunmasındaki etikisi gözlemlenmiştir. İki ay sonunda SF:PLLA (1:3 w/w) ve SF:PLLA (3:1 w/w) doku iskelelerindeki kalan ağırlık oranlarının enzim varlığında ve enzim olmadan %50'den fazla olduğu gözlemlenmiştir. SF:PLLA (3:1 w/w) doku iskelelerinde enzim varlığında daha fazla bozunma olmuştur.

FTIR spektrumlarına göre iki çeşit doku iskelesinde de metanol etkisi görülmüştür. SF:PLLA (1:3 w/w) doku iskelelerinde proteinin amid I ve amid II bölgelerinde SF:PLLA (3:1 w/w) doku iskelelerinde ise sadece amid I bölgesinde absorpsiyon piklerinin metanol etkisi ile farklı dalgaboylarında oluştuğu görülmüştür. Fibroin proteininin metanol ile etkileşimi ardından beta tabakaları yapılarının artışı sağlanarak suda çözünmeyen doku iskeleleri elde edilmiş ve sonraki analizlerde kullanılmıştır.

Mineralizasyon testi bir ay sürecinde SBF içinde uygulanmış ve bu süreçte doku iskelelerinin ağırlık değişimleri gözlemlenmiştir. Solüsyonda apatit kristallerinin oluşumu ve polimerlerin bozunması eş zamanlı olduğundan polimerlerdeki ağırlık değişimi sadece mineral oluşumu hakkında bilgi vermemektedir. Bununla beraber 3xmSBF konsantrasyondaki solüsyonda bir ay boyunca inkübe edilen doku iskelelerin ağırlıklarında azalma gerçekleşmiştir. Diğer yandan, 1xmSBF solüsyonunda inkübe edilen doku iskelelerin bir ay sonunda ağırlıklarında artış görülmüştür. Fakat, peptit immobilizasyonunun doku iskelelerinde ağırlık değişimlerine bir etkisi gözlemlenememiştir.

SEM görüntüleri ve atomik Ca/P oranları, mineralizasyonun 2, 3 ve 4. haftalarındaki örnekler üzerinden elde edilmiştir. SEM görüntülerine göre, örneklerin 1x ve 3xmSBF solüsyonlarında 2.hafta inkübasyonu ardından peptit içeren ve içermeyen formlarında mineral oluşumu gözlemlenmiştir. 1xmSBF solüsyonunda inkübe edilen doku iskelelerinde Ca/P oranları hesaplanmıştır. 3. ve 4. hafta mineralizasyonu ardından yüzeylerde daha fazla kalsiyum birikimi sonucu kalsifikasyon saptanmıştır. İki çeşit doku iskelesinde de 3.ve 4. haftada mineralizasyon ve ayrıca kalsifikasyonun arttığı görülmüştür. 4. hafta mineralizasyon sonrası 1xmSBF solüsyonundaki peptit içeren SF:PLLA (3:1 w/w) ve 2.hafta mineralizasyon sonrası peptit içeren SF:PLLA (1:3 w/w) doku iskelelerindeki Ca/P oranları hidroksiapatitin sitokiyometrik değerine (1.67) yakın değerlerde bulunmuştur.

FTIR spektrumları sadece 3xmSBF solüsyonunda inkübe edilen peptit içermeyen örnekler için alınmıştır. Poli (l-laktik asit) polimerinin karakteristik grupları ile HAp kristallerinin gruplarının benzer bölgelerde olması yüzünden değişimlerin ayırt edilmesi zor olmuştur. Yine de CO_3^{-2}, PO_4^{-3}, tip A ve B karbonat (CO_3HAp) ve OH^- gibi HAp kristallerine ait olan grupların absorpsiyon pikleri özellikle mineralizasyonun ilk haftası sonrasında saptanmıştır.

Osteoblast hücrelerinin (hFOB) doku iskeleleri üzerindeki tutunmaları, 1, 4 ve 7. günlerdeki MTS analizi ile gözlemlenmiştir. SF:PLLA (3:1 w/w) doku iskelelerinde, SF:PLLA (1:3 w/w) formlarına göre daha fazla hücre tutunması görülmüştür. Ayrıca, peptit dizisi içeren SF:PLLA (1:3 w/w) formların peptit dizisi içermeyen iskelelere göre daha fazla hFOB hücre tutunması gerçekleşmiştir. Ayrıca, SF:PLLA (3:1 w/w) doku iskelelerinde peptit dizisi içeren formlarda daha düşük hücre tutunması gözlemlenmiştir.

Sonuç olarak, mineralizasyon sürecini etkileyelebilecek peptitler kullanılarak liyofilizasyon yöntemi ile kemik yapısına benzer iki farklı konsantrasyonda kompozit doku iskeleleri elde edilmiştir. Peptit immobilizasyonu, mineralizasyon ve hücre tutunmasına etki etmiştir ama her zaman pozitif sonuç alınamamıştır. İleriki çalışmalarda, polimerlerin yüzeyinde peptit dağılımlarını gözlemleyebilmek için işaretli peptit dizileri kullanılabilir. Ayrıca immobilize olan peptitlerin konsantrasyonunun optimizasyonu için HPLC analizi yapılabilir. Ek olarak, kalsiyum birikimini gözlemlemek için *von Kossa* boyaması uygulanabilir. Sonuç olarak, peptitlerin etkilerini daha iyi anlayabilmek ve optimize edebilmek için daha kapsamlı bir çalışma gerekmektedir.

1. INTRODUCTION

1.1 Purpose of Thesis

Tissue engineering field has been growing up in every year to deal problems associated with tissues and organ failures that occur in human body because of damages after illness or accident. Tissue engineering is a multidisciplinary area, which includes chemistry, biology and engineering techniques to acquire new materials to be used as tissue or organ replacements.

To mimic natural tissues, various materials are used such as metals, ceramics, bioactive glasses, composites and polymers. Additionally, different properties should be considered when fabricating microenvironments for cells to trigger tissue regeneration. These properties, such as biocompatibility, biodegradation or non-immunogenicity, are essential and generally easily obtained with tailor made polymeric materials. Natural and synthetic polymers are widely used in tissue engineering to form porous, degradable scaffolds that also promotes cell attachment and proliferation with ideal microenvironments in various tissues like bone, skin, cartilage or liver during regeneration.

In this study, poly (l-lactide acid) and silk fibroin, as synthetic and natural polymers respectively, were used in two different concentrations to obtain porous, biodegradable, biocompatible scaffolds that enable the induction of mineralization for bone tissue regeneration. A 13 amino acid sequence (OSN) that is present in the osteocalcin protein with amidic form was immobilized on polymer surfaces via carbodiimide chemisty. The characterization tests such as water uptake, biodegradation, biomineralization and cell viability were applied to investigate the effect of peptides and different polymer concentrations.

1.2 Tissue Engineering

To figure out problems, investigate and create remedies in healthcare, multidisciplinary fields including cellular, tissue engineering and biomedical

engineering are constantly evolving in every year (Langer and Tirrell, 2004). In case of diseases or crashes, deformation or losing functions on tissues, limited supply of donors and organ failures may be occurs (Langer and Vacanti, 1993). Tissue engineering, a growing special field in regenerative medicine, includes biomaterials with the purposes of various constructions that similar to natural in managing cell functions and guidance of new tissue formation (Kundu et al., 2014). Tissue engineering is associated with participating disciplines to generate studies with building blocks such cells, biomaterials and bioreactors (Figure 1.1) (Birla, 2014).

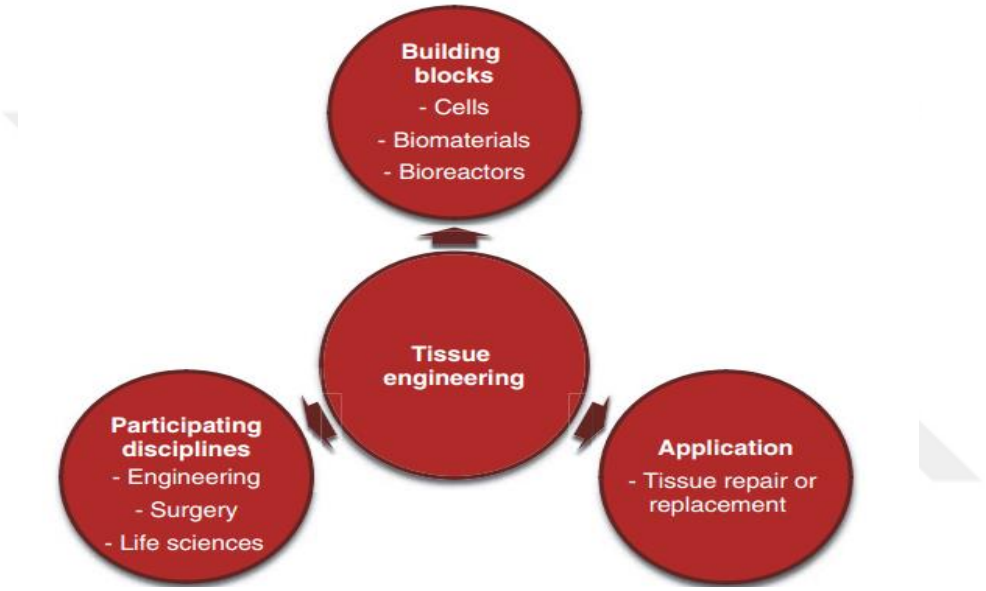

Figure 1.1: Main description of tissue engineering (Birla, 2014).

This field aims to form new structures to replace any tissue, improve tissue function, self-renewal and interact within biological systems in harmonization (Dzhoyashvili et al., 2015). Various kind of studies gradually increase and expand in bioengineering tissues of liver, nerve, skin, bone, cartilage and ligament etc. (Chen et al., 2002). Application procedure begins with biodegredable scaffold production and culturing of cells into these 3D scaffolds to perform new tissue or organ (Hutmacher, 2001). During extracellular matrix produces from cells, scaffolds has been degraded and replaced by new formed tissue (Figure 1.2). In this cascade, these structures should allow to cell migration, delivering biochemical factors, diffusion of nutrients and deported products from microenvironment (Patel et al., 2011).

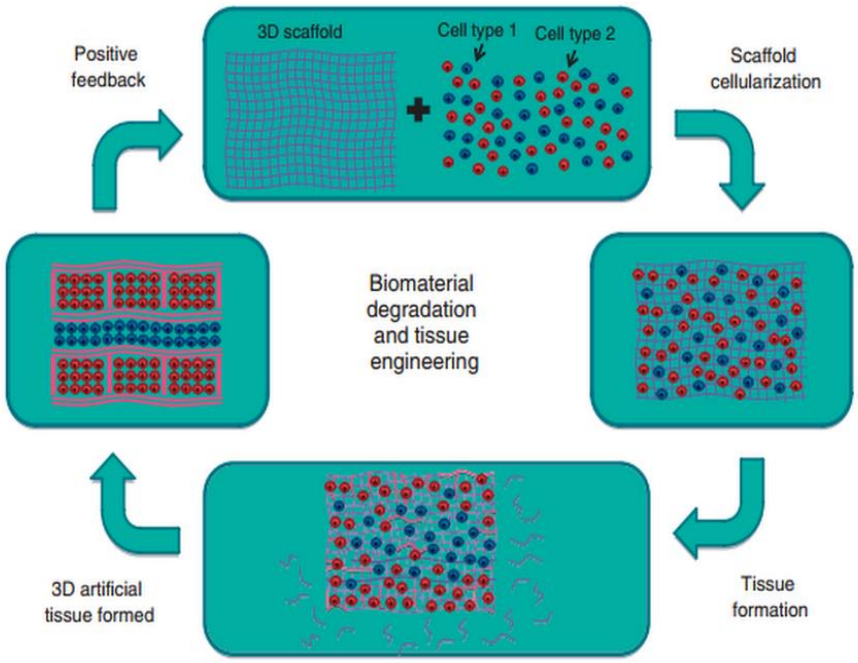

Figure 1.2: Stages of tissue formation via 3D scaffold.

While designing new temporary scaffolds, important point should be considered that a compatible microenvironment for cell adherence, differantiation, proliferation and secretion of their own cellular matrices (Nerem and Sambanis, 1995). These optimum scaffolds have also excellent characteristic properties such as biocompatibility, biodegradable, reproducibility, favorable porosity, non-immunogenic, non-toxic and stable mechanical propertities for successfully treatments (Corin and Gibson, 2010).

With this purposes, a lots of materials such as ceramics, alloys, and metals, natural and synthetic polymers are used in tissue engineering with diverse forms like films, hydrogels, bioglasses, scaffolds, granules and fibers (Langer and Tirrell, 2004). According to desired properties for constructions like cartilage, bone, ligaments, skin, epithelium, vascular graft, hepatic or cardiac, materials are choosed and processed in alone or hybrid two or three dimensional systems (Do, 2015; Gieseck, 2014). In this kind of system, an issue that should be considered, promoting cell attachment, proliferation, colonization and differentiation, extracellular matrix synthesis and vascularization with bioactive growth factors especially for embrionic and adult stem cells, stem-like progenitors in particular structure (Eberli, 2011).

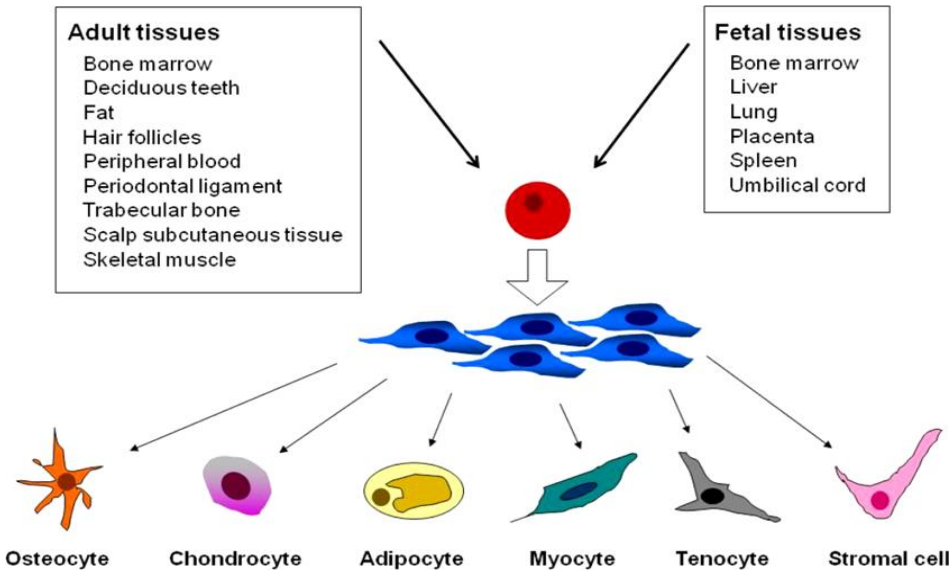

Figure 1.3: Source of mesenchymal stem cells and multipotent differentiation capacity (Eberli, 2011).

To obtain cell differentiation during tissue regeneration, transforming growth factor beta-1 (TGF-β1), insulin like growth factor (IGF), vascular endothelial growth factor (VEGF) and etc. are frequently used (Figure 1.3). The bioengineered scaffolds provide optimum microenvironments for cell differentiation and regeneration of various tissues (Gnecchi, 2008).

1.2.1 Bone tissue engineering

Bone is a specialized connective tissue, which includes major components like hydroxyapatite and collagen type I (Griffith and Naughton, 2002). The mechanical strenght of bone tissue is important feature for withstanding loads, therefore bone tissue demands biomaterials to have this physicological role at defect site (Shrivats, 2014). For bone formation as similar nature structure, have controlled degradable time, specific robustness belongs to region and enable to matrix deposition via biocompatible feature for cells are essential issues in bone tissue engineering.

Biomaterials can be classified precisely into organic and inorganic materials that preparing from natural and synthetic components. Generally, naturally derived biomaterials such as collagen, silk, hyaluronic acid, alginate and chitosan have advantages like biocompatibility, ensuring cell adhesion and migration, osteoconductivity than synthetic materials. On the other hand, difficulties in reprocessing and purification of materials from natural sources are limitations in use of natural polymers (Epstein, 2011). For having mechanical strenght as similar with

natural bone tissue and processing desirable architectural construction at regenerate site, various polymers such as polyglycolic acid (PGA), polylactic acid (PLA), polycaprolactone (PCL), polyethylene (PE), poly(methy methacrylate) (PMMA) are frequently synthesized and used in bone tissue engineering. Despite of easily available sources of synthetic polymers like amino acids, polyethers, polycarbonates via polymerization, lack of bioactivity in host-construction interactions of these materials leads to design hybrid systems from both natural and synthetic materials for gathering required properties (Kim et al., 2012; Hafeman et al., 2008).

These kinds of polymer constructions in bone regeneration should have osteoconductivity, osteoinductivity for osteogenic lineages. In bone defect regeneration, process includes osteoblasts, mesenchymal cells migration and attachment on surfaces of polymers and differentiations of stem cells are important. Additionally, several components including osteopontin, osteonectin, osteocalcin proteins are synthesized in new tissue during osteogenesis period (MacIntosh, 2008).

1.3 Bone Structure

Bone structure has two special components as organic and inorganic. To understand how bone growths, remodels, two components of bone should be investigated. An extracellular matrix as a large part consist of collagen type I and 70% inorganic mineral (hydroxyapatite). An organic matrix and water exist with 25% and 5% concentrations, respectively in calcified bone (Liu, 2016).

The mineral phases are present in bone with different calcium phosphate ratios as tricalcium phosphate (TCP-$Ca_3 (PO_4)_2$), dibasic calcium phosphate (DCP-$CaHPO_4$), dicalcium phosphate ($Ca_2P_2O_7$) and hydroxyapatite (HAp-$Ca_{10} (PO_4)_6 (OH)_2$) which is a significant major crystal compound and amorphous phase (ACP) (Park, 1984).

1.3.1 Hydroxyapatite (HAp) formation

Hydroxyapatite has a high crystalline and a greater chemically and thermodynamically stable structure in human body temperature and pH (37 ℃ and 7.4) (Neuman and Neuman 1958).

The hydroxyapatite has the molecular structure of apatite that includes calcium (Ca^{2+}), phosphorus (P^{5+}) and hydroxyl radical (OH^-) (Figure 1.4). And this

stoichiometric hydroxyapatite has a specific Ca/P ratio as 1.67 value (HAp crystalline), also contains CO_3^{2-}, Mg, Na, Cl and F ions. The amount of ions effect on the degree of crystallinity and bioactivity of structures.

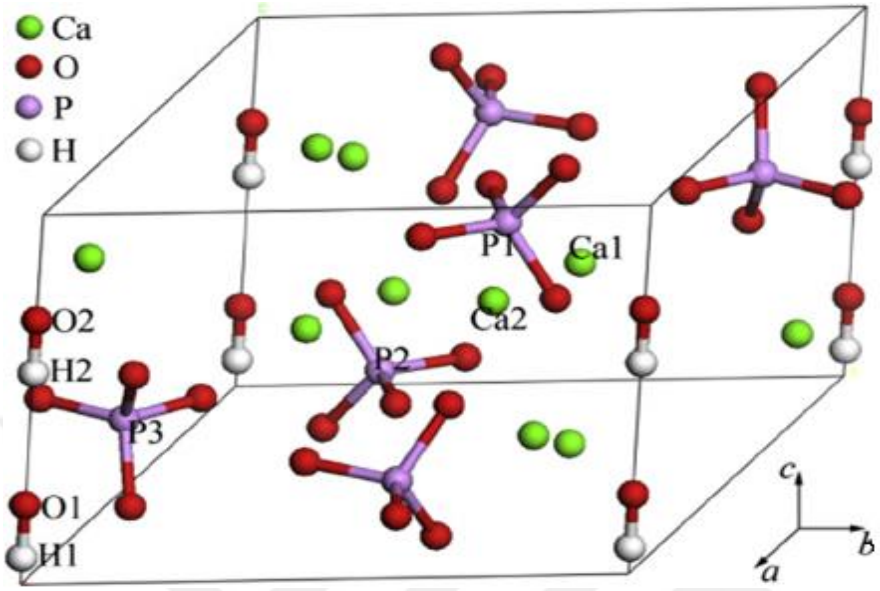

Figure 1.4: Crystalline structure of hydroxyapatite (Ren et al., 2013).

Different methods have been reported to synthesize hydroxyapatite as solid-state synthesis at high temperature, synthesis in aqueous phase, sol-gel and chemical methods, plasma spray methods etc. (Chae, 1992; Dhert, 1991). In order to mimic reproducible apatite formation in vitro, simulated body fluid (SBF) was developed as similar with biological environmental. A few kind of simulated body fluids are used with difference amounts of reagent-grade salts buffered at optimum pH and temperature (Palmer, 2008).

SBF has similarity with blood ion concentration and helps to accumulate calcium and phosphorus ions on surfaces of biomaterials. At this microenvironment, apatite crystals grow up from amorphous calcium phosphates structures. It has been reported that polymer materials (crystallinity, hydrophobicity/hydrophilicity of the surface), the porous structure (pore size, shape and interconnectivity) and ion concentrations of SBF effects to growth of apatite crystals (Zhang and Ma, 2004).

Additionally functional groups such as COOH and OH help to increase nucleation of apatite during the mineralization process (Zhang and Ma, 1999).

1.4 Synthesis of Tissue Engineering Scaffolds

1.4.1 Scaffold fabrication techniques

The scaffolds for bone tissue engineering must be tuned in many aspects to conform desirable features. Some properties like porosity, interconnectivity, degradation rate, surface chemistry, mechanical strenght etc. should be considered in order to provide a suitable microenvironment for cell attachment, proliferation, synthesis of matrix proteins and mineralization (Liu and Peter, 2003). In recent years, many techniques that include electrospinning, particulate leaching, gas foaming, rapid-prototyping, phase separation, self-assembly and freeze drying are commonly used for different functional scaffolds (Patel et al., 2011).

1.4.1.1 Particulate leaching technique

The particulate leaching technique involves the porogens such as salt, sugar particules that uses for obtain sponge/foam-like scaffolds. To design constructions with desirable pore sizes, the porogens are used in different sizes and concentrations. During this process, the selected particules are dispersed into a polymer solution; subsequently mixture is cast into a mold. The solvent is evaporated by lyophilization and particules are leached out from scaffolds with incubation in distilled water for the required time (Edwards, 2004). To observe three-dimensonal scaffolds, various particle sizes of salts were used with different concentrations of silk fibroin and the effects on swelling ratios, porosities were reported for cartilage formation (Kim et al., 2004). Based on the desirable pore sizes, three kinds of pore sizes were studied on PLLA scaffolds in Teflon molds than supported by micro-computed tomography datas (Shastri et al., 2000).

1.4.1.2 Phase separation

To construct porous polymer membranes, phase separation method is used and versatile depending on polymer and concentration of polymer, solvent and cooling parameters (Zhang et al., 2001). A homogeneous emulsion of polymer-solvent mixture becomes thermodynamically unstable and separated into liquid-liquid and solid-liquid phases (Chen et al., 2002). PLLA uniform foams were constructed from homogeneous naphthalene solutions and releasing of drugs and nutrients were investigated from porous foams (Lo et al., 1996).

1.4.1.3 Gas foaming process

This technique is used to obtain highly porous polymer structure without using any organic solvent. The polymer disks are exposed to high-pressure carbon dioxide (CO_2) gas for saturation. Then, the gas is rapidly released from polymer structure by the helping of thermodynamic instability (Patel et al., 2011). However, this technique cannot provide interconnective pores in structucture and even closed-pores are created which are not compatible for cell proliferation or diffusion nutrients (Liu and Peter, 2003).

1.4.1.4 Rapid-prototyping techniques

The complex scaffolds can be designed with this rapid-prototyping method. This method based on the advanced development of computer science and computer-aided design (CAD) model is used to produce complex structures. The operation parameters such as drop position, flow rate and speed can be controlled depending on the desired scaffold. On the other hand, this technique is not efficient to generate microstructures (Yang et al., 2002).

1.4.1.5 Electrospinning technique

The scaffolds that composed from nanometer fibers are fabricated with electrospinning process. These fibrous scaffolds can be obtained with fiber diameters in several microns down to several hundred nanometers (Li et al., 2002). The microporous structures are famous for the cell proliferation, attachment and migration. Therefore, electrospining tecnique is widely used in tissue engineering. Briefly, the polymer solution is injected and electical potential is applied to this solution in charge imbalance. The charge imbalance overcomes to surface tension and provides solvent evaporates and creates polymer fibers. The silk nanofiber scaffolds were observed with different electrospinning parameters as voltage, flow, rate, distance between syringe and plate (Liu and Peter, 2003).

1.4.1.6 Self-assembly

The self-assembly process is widely used for fabrication of various nanofiber structures. In this process, the biological components can be self-assembled by weak covalent or hydrophobic interactions, electrostatic interactions, van der Waals, ionic

or hydrogen bonds. For instance, many different proteins and various peptides talent to be self-assembled nanofibers and create three-dimensional microenvironments for cell attachment, migration (Hartgerink et al., 2001). In a study, conformational transition of silk fibroin were tuned between random coil and beta sheet form in the presence of Ca^{2+} ions and analyzed the changes in mechanism of self-assembly fibroin process by circular dichroism (Dubey et al., 2015).

1.4.1.7 Freeze drying

Freeze-drying process is a convenient technique to fabricate highly porous scaffolds. This process consists of three main steps. At the first step, homogenous solvent-polymer solution is freezed at a desired low temperature such as -20℃, -80℃ etc and solvent is prefreezed as ice crystals. In other steps, the frozen samples are placed into a lyophilizer with under the low pressure and temperature conditions. The main drying occurs by sublimation process, which includes the evaporation of ice crystalls of solvent. Then, the final drying is applied with increasing pressure and temperature and results in the formation of ice crystals. Finally, the solvent is removed from polymer structure and porous scaffolds are observed (Lu et al., 2013).

The pore sizes, porosity ratio and distribution of pores can be controlled by prefreezing conditions to fabricate micro and nano structures. During the freezing step, the ice crystals grow and solute polymer molecules are excluded from crystals. Under the extremely low temperature, ice nucleation occurs rapidly and results into large ice crystals. However, under the high freezing temperature, ice nucleation is slow and small ice crystals are formed (Qian and Zhang, 2010).

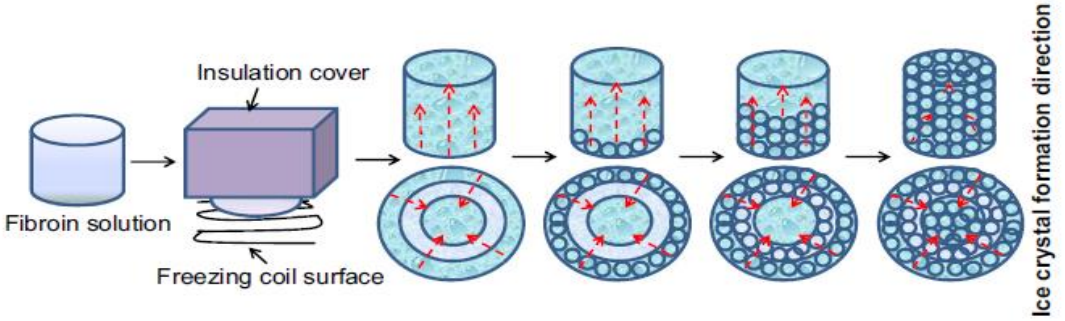

Figure 1.5: Schematic representation of freezing method employed for directional ice crystal formation within 3D silk fibroin scaffolds (Qian and Zhang, 2010).

The three dimensional silk fibroin scaffolds were fabricated by directional freezing process (Mandale and Kundu, 2009). In this study, the freezing was slowed and the direction of ice crystal growth was determined by insulation cover (Figure 1.5). The ice crystals were uniformly placed and homogeneous pore formation was obtained in structures for dermal fibroblasts proliferation and migration.

1.5 Natural and Synthetic Polymers

The last three decade of twentieth century shows frequently usage of biodegradable biomaterials (enzymatically or hydrolytically degradable) than biostable biomaterials. The advantages of biodegradable materials are non-toxic, elastic and biocompatible properties. They can be easily modified, enable to replace with natural tissue and not required second operation after implantation inside a living body (Shalaby and Burg, 2003).

These biodegradable polymers are obtained from natural sources or synthesized by chemical reactions. Protein origin polymers (collagen, gelatin, fibroin) and polysaccharides (chitosan, alginate, hyaluronan) are used as natural polymers and polyhydroxyalkanoates, poly (glycolic acid), poly (L-lactide acid), polycaprolactone, poly(urethane)s, polyanhydrides etc. These kind of biodegradable polymers can be easily modulated according to the various desired tissues in regenerations than metals, alloys or ceramics (Patel et al., 2011).

1.5.1 Silk fibroin protein

Silks are synthesized by different species of silkworms and spiders. According to the species of silkworms or spiders, properties of silk fibers changes such as diameter, molecular weight, elasticity and especially ratio of secondary structures such as β-sheet, random coil and α-helix structures which effects on solubility and mechanical strenght in protein (Liu et al., 2013). Depending on the target tissue, the silk protein with appropriate properties can be selected for scaffold production.

Silk proteins (polyamino acids) are secreted by Saturnidae and Bomycidae insects and essential components of cocoons. The silkworm cocoons, *Bombyx mori* cocoons, are constructed with twin threads by Bombucidae family and these kinds of cocoons has sericin protein as protective cover (Mondal et al., 2007).

The silk gland cells of silkworm synthesis the liquid silk and drives out into fibers during spinning (Chavancy et al., 2005). Silk protein consists of two different proteins, fibroin which presents in the inner layer of cocoons and sericin, which coats the structure in the outer layer (Figure 1.6) (Gerritsen, 2002).

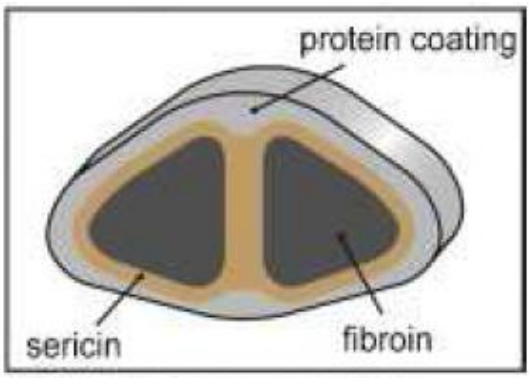

Figure 1.6: Schematic illustration of *B.mori* silk structure which is constructred by two brain of fibroin and sericin as coating protein in cocoons (Gerritsen, 2002).

Sericin protein is useful with special properties such as antibacterial UV resistant, absorb and release moisture, resist oxidation etc. (Mondal et al., 2007). This protein easily hydrolyzed, dispersed and removed from other components in hot water if degumming process carries out. Silk fibroin protein is obtained by degumming process of cocoons (Rockwood et al., 2011). The amount of components in *B.mori* cocoons as shown in Table 1.1 and fibroin protein presents as a major constituent in cocoons (Gulrajani, 1988).

Table 1.1: Compositon of silk in *Bombyx mori* (Gulrajani, 1988).

Component	%
Fibroin	70-80
Sericin	20-30
Wax matter	0.4-0.8
Carbonhydrates	1.2-1.6
Inorganic matter	0.7
Pigment	0.2
Total	100

B.mori silk includes three proteinaceous complex structures: a heavy chain fibroin (*H-chain*, 350kDa), a light chain fibroin (*L-chain*, 25kDa) and small glycoprotein known as the P25 protein (P25, 30kDa). The molar ratios of H-chain: L-chain: P25 are 6:6:1 The H-chain is more hydrophobic and the L-chain is more hydrophilic and elastic. P25 protein presents as a protective on integrity of complex (Tanaka et al.,

1999). The amino acid composition of silk fibroin is classified according to heavy and light chains as shown in Table 1.2 (Shimura et al., 1982).

Table 1.2: Amino acid composition of *B. mori* fibroin (Shimura et al., 1982).

	Composition, mol %		
Amino acid	Total	Heavy areas	Light areas
Glycine	42.9	49.4	10.0
Alanine	30.0	29.8	16.9
Serine	12.2	11.3	7.9
Tyrosine	4.8	4.6	3.4
Valine	2.5	2.0	7.4
Aspartic acid	1.9	0.65	15.4
Glutamic acid	1.4	0.70	8.4
Threonine	0.92	0.45	2.8
Phenylalanine	0.67	0.39	2.7
Methionine	0.37	-	0.37
Isoleucine	0.64	0.14	7.3
Leucine	0.55	0.09	7.2
Proline	0.45	0.31	3.0
Arginine	0.51	0.18	3.8
Histidine	0.19	0.09	1.6
Lysine	0.38	0.06	1.5

The glycine, alanine, serine and tyrosine amino acid residues have large mole fraction (90%) in fibroin and repeated sequence represented by general formula as shown below: (Valluzzi and Gido, 1997).

-Gly-Ala-Gly-Ala-Gly-Ser-Gly-Ala-Ala-Gly-[-Ser-Gly-$(Ala\text{-}Gly)_n$-]$_8$-Tyr-

The supramolecular interaction of hydrogen bonding between amino acids or π interactions between aromatic groups, determines the secondary structure of fibroin polymer. To modulate the secondary structure of fibroin for desired scaffolds, some treatments are applied which effects on soluble/insoluble properties such as water annealing process, chemical treatment with methanol or ethanol solvents (Figure 1.7) (Jin et al., 2005).

The natural silk fibroin structure has different ratios of random coil, alpha helix and beta sheet structures that effect on solubility of protein. When the random coil structure present with higher concentration in fibroin, the protein is more soluble in their forms. When increasing beta sheet conformation, the protein is more insoluble after treatments (Jin et al., 2005).

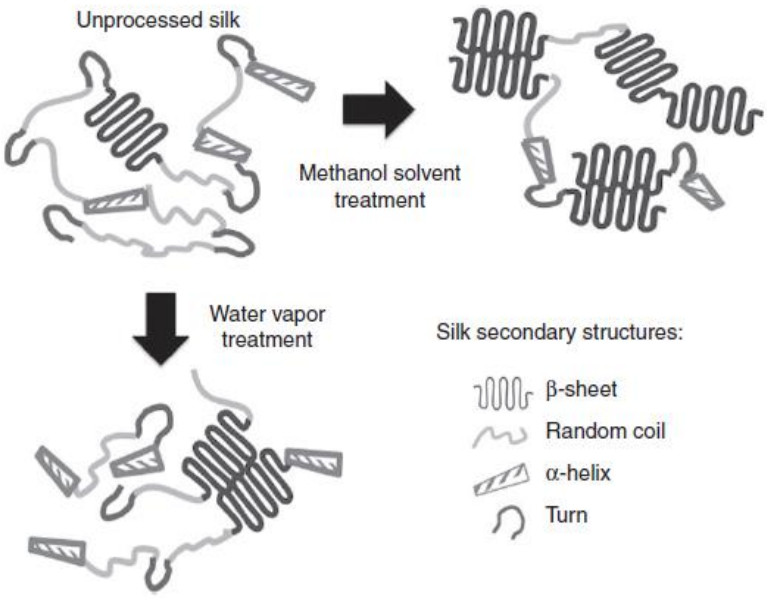

Figure 1.7: An illustration on changes in secondary structure of fibroin during treatments (Jin et al., 2005).

In tissue engineering, silk fibroin is frequently used in recent years because of the ideal properties such as low inflammatory potential without sericin, biocompatibility, high tensile strenght, flexibility, controlled biodegradation and so on (Altman et al., 2002). As a natural material, silk fibroin is processed into various types of structures: electrospun fibers, sponges, microspheres, hydrogels and films. The silk fibroin films (after water vapour and methanol treatment) support the growth of osteoblasts in bone tissue engineering (Jones et al., 2009). In another study, silk fibroin combined with low crystalline hydroxyapatite and obtained ideal scaffolds to promote osteogenesis and regenerate bone/ligament defects in rabbit models (Shi et al., 2013). Additionally, some modification techniques are used such as apatite and BMP-2 integration to generate higly porous scaffolds to increase osteoconductivity (Kim et al., 2008). The various fibroin sponges were also obtained with different freezing conditions due to observe homogen porosity and mechanical strenght for good cell migration and proliferation (Qian and Zhang, 2010). On the other hand, electrospun nanofibers are generated with desired dimensions and crystallinity, tensile strenght properties in bone tissue engineering (Andiappan et al., 2013).

1.5.2 Poly L-lactide acid (PLLA)

The lactide is a chiral polymer and exist in two optically active forms: D-lactide and L-lactide. After polymerization of these monomers result into semi-crystalline

polymers. L-lactide is a naturally occuring isomer and has 37% crystallinity. But the degradation time and degree of crystallinity depends on the molecular weight and processing parameters (Middleton and Tipton, 2000).

PLLA polymer is approved by FDA (Food and Drug Administration) for special clinical applications. It has been used as orthopedic implants and still frequently choosed and combined with other polymers to acquire desired properties in bone tissue engineering (Saito et al., 2013). This polymer is easily available, bioresorbable, biocompatible material and fabricated with desired porosity and mechanical properties. Additionally, PLLA has long shelf life and easy to sterilize. On the other hand, PLLA has disadvantages with low cell integration, low mechanical strenght and rapid biodegradation (Dzhoyashvili et al., 2015). The different degrees of hyrophobiliciy and ratio of lactid acid effects on biodegradation behaviour (Kaushiva et al., 2007; Li et al., 2006). A many forms of PLLA are choosed in bone tissue engineering such as films, sponges, nanofibers.

In a study, PLLA and chitosan composite scaffolds were obtained by three different techniques (solvent-extracting, freeze-drying and liquid-solid separation) and interconnective porous structures and controllable porosities were acquired (Wan et al., 2007). Additionally, some peptides are integrated into PLLA scaffolds to increase biocompatibility. For example, immobilization of RGD in PLLA scaffolds promoted cell attachments on surfaces (Ho et al., 2006). In another study, addition of recombinant BMP-2 proteins into PLLA scaffolds increased biocompatibility and regenerative capacity (Chang et al., 2007). In addition, nanofibrous PLLA scaffolds that combined with other polymers such as caprolactone and silk fibroin were studied in tissue engineering (Zhang et al., 2009).

1.6 Peptide Immobilization

To improve the properties of biomaterials for good cell attachment, increase bioactivity, mineralization and mimic the native tissues, surfaces of biomaterials are modified with various peptides by chemical or physical immobilization techniques (Hennessy et al., 2009). Especially, addition of hydophilic polymers into the structure or immobilization of hydrophilic peptides or ions on surfaces are most preferred in tissue engineering. After these modifications, the scaffolds can be more

hydophilic to promote cell adhesion and differentiation and more biodegradable than before (Kim et al., 2010).

Several various peptide sequences are frequently used in tissue engineering to improve surfaces of polymers. The essential proteins of natural bones such as bone sialoprotein (BSP), osteopontin (OPN) and osteocalcin are used as sources for generation of peptide sequences, which include desired lenghts and amino acid composition (Fujisawa and Kuboki, 1992). Fmoc synthesis procedure (solid phase synthesis) technique is generally used for generation of various peptide sequences (Itoh et al., 2002). For example, immobilization of Arginine-Glycine-Aspartic acid (RGD) peptide sequence on chitosan surfaces increased biocompatibility for osteoblast-like cells. In another study, Arginine-Alanine-Aspartic acid-Alanine-16 (RADA-16) peptide, as a well known self assembly sequence, was used to coat fibroin scaffolds and resulted in higher biomimetic nanofibrous scaffolds and increased ligament regeneration (Chen et al., 2012). A collagen-binding motif (CBM) was isolated from OPN, showed increase bone formation in vivo and promoted osteogenesis (Lee et al., 2007). Bone morphogenetic protein-2 (BMP-2) derived peptides are also choosed to promote osteoinductivity potential of scaffolds (Jeon et al., 2007; Qiao et al., 2013). A many of peptide immobilization studies are available depends on requirements in bone tissue engineering.

1.6.1 HAp-binding peptides

The mineralization process is important for bone regeneration and cellular mechanisms according to the extracellular matrix deposition. To induce mineralization during regeneration, special peptides are used which have higher affinity to hydroxyapatite crystalls. In recent years, hydroxyapatite-binding peptides are synthesized from natural bone proteins or synthetically produced with Fmoc or Phage Display method (Roy et al., 2008).

In a study, RGD sequenced was modified with glutamic acid sequence (E_7-RGD) because of glutamic acid have a high affinity to hydroxyapatite and resulted in increase osteoblast differentiation (Itoh et al., 2002). In another study, P-15 amino acid sequence, which was obtained from Type I collagen, enhanced viable cell attachment and migration and promoted matrix mineralization (Thorwarth et al., 2005; Hanks and Atkinson, 2004). To promote mineralization *in vitro* for PLGA-

PEG copolymer surfaces, BMP-2 derived osteoinductive peptide (designated P24) was used and observed higher calcium deposition than control samples after 14 days (Pan et al., 2014).

Osteocalcin-derived peptides are used in bone tissue engineering. Hosseini *et al.* revealed a 13 amino acid peptide sequence (LEPRREVCELNPD) which is synthesized from first helix of osteocalcin protein and has high affinity to HAp (Hosseini et al., 2013). The acidic (OSC) and amidic (OSN) forms of this peptide were studied to observe the effects of peptide presence on mineralization rate as shown below:

OSC peptide sequence:

Leu-Glu-Pro-Arg-Arg-Glu-Val-Cys-Glu-Leu-Asn-Pro-Asp-OH (free C-terminal acid form)

OSN peptide sequence:

Leu-Glu-Pro-Arg-Arg-Glu-Val-Cys-Glu-Leu-Asn-Pro-Asp-NH_2 (amidated C-terminal form)

The circular dichrosim experiments indicated that conformational changes of peptides resulted in interaction with calcium and phosphates (Hosseini et al., 2014). To improve surface bioactivity of stainless steels, OSN peptides were immobilized by physical adsorption on surfaces. This study showed OSN peptides promoted more apatite crystal formation from amorphous calcium phosphates than OSC peptides after two hours and proved the effect of peptide on nucleation during mineralization on stainless steel. On the other hand, there is no available study that shows the effect of OSN peptides on polymer scaffolds to enhance biomineralization.

In this study, OSN peptides were immobilized on PLLA/fibroin composite scaffolds to promote HAp nucleation and rapid mineralization for improvement ideal scaffolds in bone tissue engineering.

2. MATERIALS AND METHODS

2.1 Materials

2.1.1 Chemicals

The list of chemicals that were used in this study and their suppliers were given in Appendix A.

2.1.2 Solutions

The solutions that were used in this study and their compositions were given in Appendix B, and Appendix C.

2.1.3 Laboratory equipment

The laboratory equipments that were used in this study were listed in Appendix D.

2.2 Method

2.2.1 Silk fibroin degumming process from *Bombyx mori* cocoons

The *Bombyx mori* cocoons were bought from Bursa Kozabirlik Cooperative. At the beginning, cocoons were cut into 0.5 cm height circular pieces, silkworms were disposed and 5 gram of cocoons were weighed. Then 2L of ultrapure water in a glass beaker was boiled and 4.24 gram of sodium carbonate (Na_2CO_3) was added to prepare a 0.02 M solution for alkali degumming. After a homogeneous solution was obtained, the cocoon pieces were added to the solution and cooked for 30 min. via stirring with a spatula to promote good dispersion of silk fibroin. At the end of the boiling, the silk fibroin was transferred to 1L of ultrapure water in a glass beaker and rinsed three times (an hour each) via changing ultrapure water. By this way, the hydrophilic sericin protein and other parts such as wax matter, carbonhydrates and pigments were separated to obtain pure fibroin protein.

The rinsed fibroin was dried on aluminium foil under fume hood overnight. The following day, the dried fibroin was dissolved in 9.3M lithium bromide solution (silk

protein to LiBr ratio of 1 to 4 w/v), a strong solvent for breaking of disulphide bonds that link heavy and light chains within fibroin. This dissolving process was done at 60°C overnight. The final solution appeared with amber colour, viscous and not included fibers.

The 3-day dialysis process was begun via transferring the fibroin solution to the dialysis cassettes after the dilution with ultrapure water at a ratio of 1 to 3, fibroin solution to water. Two dialysis cassettes were inserted in 2L of beaker with gentle stirring and the ultrapure water was refreshed twice or thrice per day for 6 times.

At the end of 3 days, centrifugation (9000 rpm, +4°C, 20 min) was applied twice to remove impurities and undissolved fibers from fibroin solution. By the degumming of 5g cocoon, fibroin solution was obtained with approximately 35-40 mL.

Eventually, the yield of fibroin solution, calculated via drying of 0.5 mL at 60°C, was generally found between 4-6% w/v. Finally, the solution was stored at +4°C up to a month until use for the next step.

2.2.2 Fabrication of composite scaffolds

The poly L-lactide acid (PLLA) polymer and lyophilized-fibroin protein were used for the preparation of composite scaffolds. 1,1,1,3,3,3-Hexafluoro-2-propanol (HFIP) is a common solvent and used to obtain a homogeneous polymer solution.

The lyophilized-fibroin was obtained by lyophilization of silk fibroin solution for 24h at -50°C. PLLA and lyophilized-fibroin were dissolved in HFIP separately without stirring at room temperature under fume hood because of the HFIP toxicity. When homogeneous solutions were observed, PLLA and fibroin solutions were mixed with magnetic stirring for a while and subsequently transferred into the 96-well plate. The ratio of PLLA to silk fibroin (SF) was either 3:1 w/w or 1:3 w/w in 3% w/v total polymer solution. The well plate was placed at +4°C for 1h and then placed at -20°C with insulation cover for prefreezing in slowly.

The lyophilization step was carried out for 60 min. at -30°C after freezing with main drying and 15 min at -20°C with final drying. For the preparation of insoluble scaffolds, methanol (97%) was added with the ratio of 1 mL methanol onto 1.7 g total polymer. During the methanol treatment, the lids of plates were closed for 30 min and after treatment, lids were opened for the evaporation of unreacted methanol

for 30 min. Then the obtained insoluble scaffolds were kept at room temperature for further characterization tests.

2.2.3. Peptide immobilization on composite scaffolds

At the beginning, carboxyl groups of polymers were activated with 1-ethyl-3-(3-dimethylaminopropyl) carbodiimide/N-hydroxysuccinimide (EDC/NHS) coupling agents. According to the total polymer concentration (3% w/v), the amount of EDC was determined (Jung et al., 2005) as $0.134x10^{-4}$ mol and the ratio of EDC/NHS was kept as 1:2 (mol/mol). The EDC/NHS coupling reaction was applied in 0.1 M 2-(N-morpholino)ethanesulfonic acid (MES) buffer (pH=5.5) at room temperature (25°C) for 4 hours with gentle horizontal shaking (25 rpm).

After first step, the samples were rinsed with distilled water for three times and immersed in OSN peptide solution. The peptide solution was prepared in 0.1 M MES buffer (pH=5.5) at 400 μg/mL. The samples were kept at +4°C during the process of immobilization by gently shaking (25 rpm) for overnight. At the following day, the samples were rinsed with distilled water for three times, dried at room temperature and used in further tests.

2.2.4 Characterization tests of composite polymer scaffolds

2.2.4.1 Water uptake test

To observe the water uptake behaviour, weights of dry samples (W_{dry}) were recorded and placed in 24-well plates. Each sample were incubated in phosphate buffer solution (PBS) at 37℃ for 24 hours. The wet weights of samples (W_{wet}) were recorded after 1 and 24 hours. The average water uptake percentages (%) were calculated with triple samples using equation 2.1:

$$\text{Water uptake ratio (\%)} = [(W_{wet} - W_{dry}) / W_{dry}].100 \qquad (2.1)$$

where W_{dry} is the weight of dry specimen, W_{wet} is the weight of wet specimen after incubation in PBS solution after 1 and 24 hour. After incubation, the samples were rinsed in distilled water and dried at room temperature.

2.2.4.2 Biodegradation test

Biodegradation process was followed for two months in the presence of protease XIV enzyme. At the beginning, the stock enzyme solution was prepared at 0.1U/mL concentration and sodium azide was added to the enzyme solution with ratio of 0.01N w/v to prevent any microbial growth on polymer surfaces. The weights of dry samples (W_o) were recorded at time 0. Then the samples were rinsed in distilled water and immersed in enzyme solution by using 24-well plate.

The degradation process was carried out at 37℃ with gentle vertical shaking (15 rpm). Enzyme solution was refreshed every two day during two months. The samples were taken at each week and rinsed in distilled water. For the control groups, the PBS solution was used without enzyme. Eventually, samples were dried at room remperature and remaning weights of samples were weighted (W_t). The percent of weight loss (%) was calculated for each sample via equation 2.2:

$$\text{Remaining weight ratio (\%)} = [(W_o - W_t) / W_o].100 \quad (2.2)$$

where W_0 is the initial weight of specimen before degradation and W_t is the remaining weight of specimen after each week periods of degradation during two months.

2.2.4.3 Biomineralization test

To observe HAp formation on polymer surfaces, biomineralization process was carried out for a month. Firstly, the modified simulated body fluid (mSBF) was prepared at pH 7.4 by NaOH titration. The OSN peptide immobilized and without peptide forms of dry samples were weighted (W_o) and rinsed in distilled water. Then both samples were placed in 24-well plates and mSBF solution was added. Two different concentrations (1xmSBF and 3xmSBF) of mSBF solution were studied. During mineralization step, mSBF solution was refreshed every two day. This process was carried on at 37℃ for a month and samples were taken at each 1, 3, 7, 14, 21 and 28th day. Eventually, samples were dried at room temperature and weights of mineralized scaffolds were recorded (W_{min}) to observe the changes of weights. The remaining weight ratios were calculated with equation 2.3:

$$\text{Remaining weight ratio (\%)} = (W_o / W_{min}). 100 \quad (2.3)$$

2.2.4.4 SEM and EDS analysis

The porosity and morphology of samples were examined via Scanning Electron Microscopy (SEM) after biomineralization and cell culture processes. The sputter coating with gold was applied on the surfaces of scaffolds to increase electrical conductivity. The HAp formation at each periods (1, 3, 7, 14, 21 and 28^{th} day) and cell attachment (1, 4 and 7 day) was observed at approximately 200x by SEM and elemental analysis was performed at 1000x magnification by EDS.

To determine the atomic ratios of calcium/phosphorus on polymers surfaces, Energy Dispersive Spectroscopy (EDS) was used for one month samples.

2.2.4.5 FTIR analysis

Fourier Transform Infrared Spectrophotometer (FTIR) was used to identify polymers with specific chemical bonds peaks and helped to detect the presence of Ca-P minerals. The spectrums were taken in region of 4000-600 cm^{-1}.

2.2.4.6 Cell viability on polymer surfaces

The peptide immobilized and without peptide forms were used for cell viability test. Human fetal osteoblastic cells (hFOB) were cultured in Dulbecco's Modified Eagle's Medium (DMEM) containing GlutaMAX supplement, 1g/L D-Glucose, and supplemented with penicillin/streptomycin (1%) and, fetal bovine serum (10%). They were incubated at 37℃ in a humidified 5% CO_2 atmosphere for proliferation. The medium was changed every two day under sterile conditions.

The scaffolds were placed in 48-well plates for 1, 4 and 7^{th} day incubation and were sterilized in 70% ethanol solution overnight. At the following day, scaffolds were rinsed with distilled water twice and immersed in 500 µL DMEM solution overnight to prepare suitable microenvironment via protein adsorption to induce cell attachment. The cells were collected at third day, centrifuged and counted with Trypan Blue dye. Subsequently, DMEM solution was removed and hFOB cells were seeded on top of the pre-wetted scaffolds ($2x10^4$ cell/scaffold). To achieve effective cell attachment, scaffolds were incubated for 4 hours at 37℃ in CO_2 incubator. Then, 500 µL DMEM solution was added to samples and incubation was carried out for 1, 4 and 7 day periods. The medium was refreshed every two days and proliferation of

cells in scaffolds were assessed by MTS assay. For that, scaffolds were transferred to another well and washed with PBS. DMEM and MTS solution, having ratio of 5:1 (500 μL solution per scaffold) was added onto the scaffolds and incubated for 2.5 hours in CO_2 incubator. After incubation, 200 μL of solution from each triple samples was transferred to 96-well plate and optical densities were measured at 490 nm using Elisa Plate Reader. Eventually, the number of proliferating cells were calculated according to the calibration curve and cell viability was calculated for each time point.

3. RESULTS AND DISCUSSION

3.1 Morphology and Chemical Structure of Scaffolds

3.1.1 The effect of insulation cover on morphology of scaffolds

After lyophilization and methanol treatment step, the scaffolds were removed from well plates and the dimensions of scaffolds were measured as 4 mm diameter, 3 $\pm$1 mm height for SF:PLLA (1:3 w/w) and 4 mm diameter, 5 $\pm$1 mm height for SF:PLLA (3:1 w/w) (Figure 3.1).

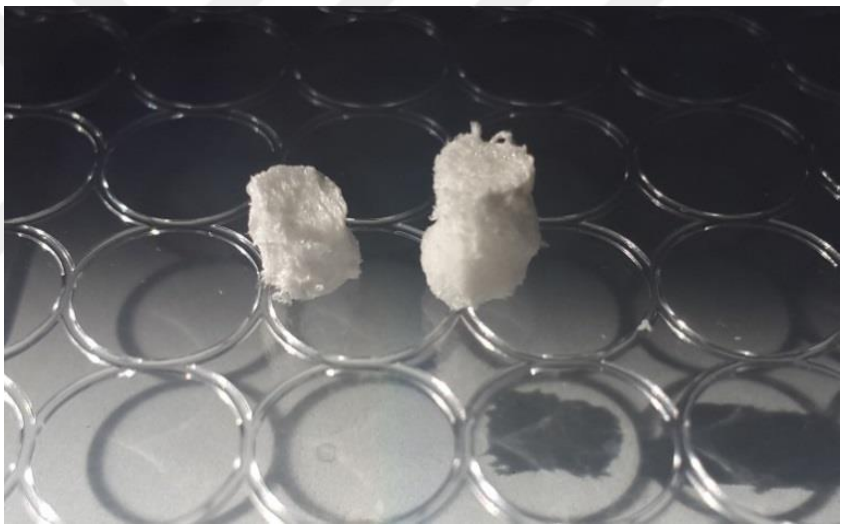

Figure 3.1: The freeze-dried scaffolds, SF:PLLA (1:3 w/w) and SF:PLLA (3:1 w/w) as shown on the left and right side, respectively.

The morphologies of scaffolds depend on various conditions such as polymer concentration, glass temperatures of polymers, freezing temperature and the control of the freeze direction (Qian and Zhang, 2010; Nazarov et al., 2004). These conditions effect the pore sizes, pore distribution and ratio of porosity. In this study, the insulation cover was used during pre-freezing time (24 hours) to obtain higher porosity (Figure 3.2). The uni-directional prefreezing provided only one directional freezing. Ice crystals growed up from the bottom of plates to up and moved from edge to the origin with using insulation cover. By the helping of this movement of ice crystals resulted in homogeneous pore distribution within scaffolds.

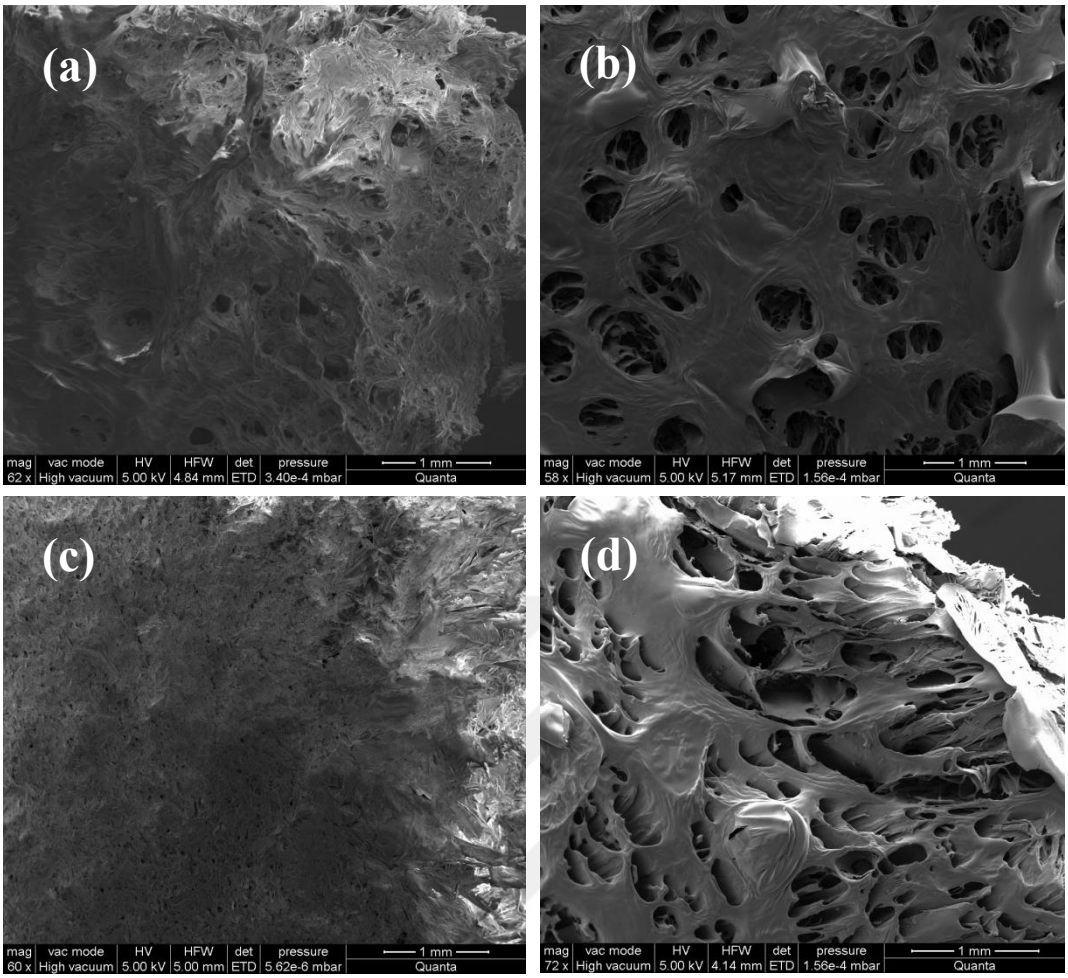

Figure 3.2: SEM images of SF:PLLA (1:3 w/w) without (a) and with (b) insulation cover, and SF:PLLA (3:1 w/w) without (c) and (d) with insulation cover.

The control of freezing direction affects the formation of homogeneous pores. The freeze drying temperatures were kept as -30℃ for main drying and -20℃ for final drying. Before freeze drying, the pre-freezing condition was changed with insulation cover and that helped to control the direction of freezing. When no insulation cover was used, only a minor porosity could be observed for both samples (SF:PLLA (1:3 w/w) and SF:PLLA (3:1 w/w)).

3.1.2 The chemical structure of scaffolds

The chemical structures of composite scaffolds were analyzed by FTIR. The secondary structure of silk fibroin can also be investigated with FTIR spectra. Silk protein has characteristic vibration bands around 1620 cm^{-1} which represent the absorption peak of peptide backbone of amide I (C=O stretching), bands around 1514 cm^{-1} to amide II (N-H bending) and the bands around 1230 and 1440 cm^{-1} to amide

III (C-N stretching) and 694 cm^{-1} to amide IV (Boccaccini and Ma, 2014; Kim et al., 2008). The molecular conformation of *Bombyx mori* silk fibroin consists of β-sheet crystalline structure (Silk II), α-helix and random coil secondary structure (Silk I). Silk I structure is non-crystalline but Silk II is highly stable and crystalline yielding insoluble protein structures (Jin and Kaplan, 2003). The characteristic absorption bands of β-sheet structure appears around 1630, 1515 and 1240 cm^{-1} and absorption bands of random coil conformation appears around 1650, 1550 and 1230 cm^{-1}. The protein secondary structure can be modulated using chemical such as methanol (MeOH) solvent, ethanol or water vapor (water-annealing) treatments. These treatments help the breakage of weak hydrogen bonds between amino acids and results in transformation of random coils to beta sheet conformation. The natural silk fibroin has difference ratio of randol coil and beta sheet structures that affect the solubility and elasticity of protein (Hu et al., 2011; Jin et al., 2005). The β-sheet structure exhibits in the spectral range 1628 to 1635 cm^{-1} (Amide I) and around 1520 to 1525 cm^{-1} (Amide II). ((Radev et al., 2013; Bunaciu et al., 2014).

After lyophilization step, the silk fibroin protein had more random coil structures and caused the soluble scaffolds. The methanol treatment induced the beta sheet conformations in fibroin protein and resulted in insoluble proteins within scaffolds. According to the FTIR results, the absorption peak at 1647.65 cm^{-1} (Amide I) was shifted to 1628.20 cm^{-1} after methanol treatment and another peak at 1533.39 cm^{-1} (Amide II) shifted to 1519.82 cm^{-1} on SF:PLLA (1:3 w/w) scaffolds (Figure 3.3). For SF:PLLA (3:1 w/w) scaffolds, the absorption peak around 1639.17 cm^{-1} (Amide I) was shifted to 1623.01 cm^{-1} after methanol treatment which showed at least a partial transformation from random coil to beta sheet conformation (Figure 3.4). When amide III regions (1230-1444 cm^{-1}) were examined, it was seen that it was hard to distinguish them since they overlap with PLLA characteristic group. Therefore, the secondary structure transformation was evaluated only in amide I and amide II region. There was no available absorption peaks observed belong to Amide III region both scaffolds.

According to the results, the randol coil structures became the beta sheet conformations partially in fibroin proteins to obtain insoluble scaffolds. The effect of methanol treatment was clearly observed with shifted absorption peaks.

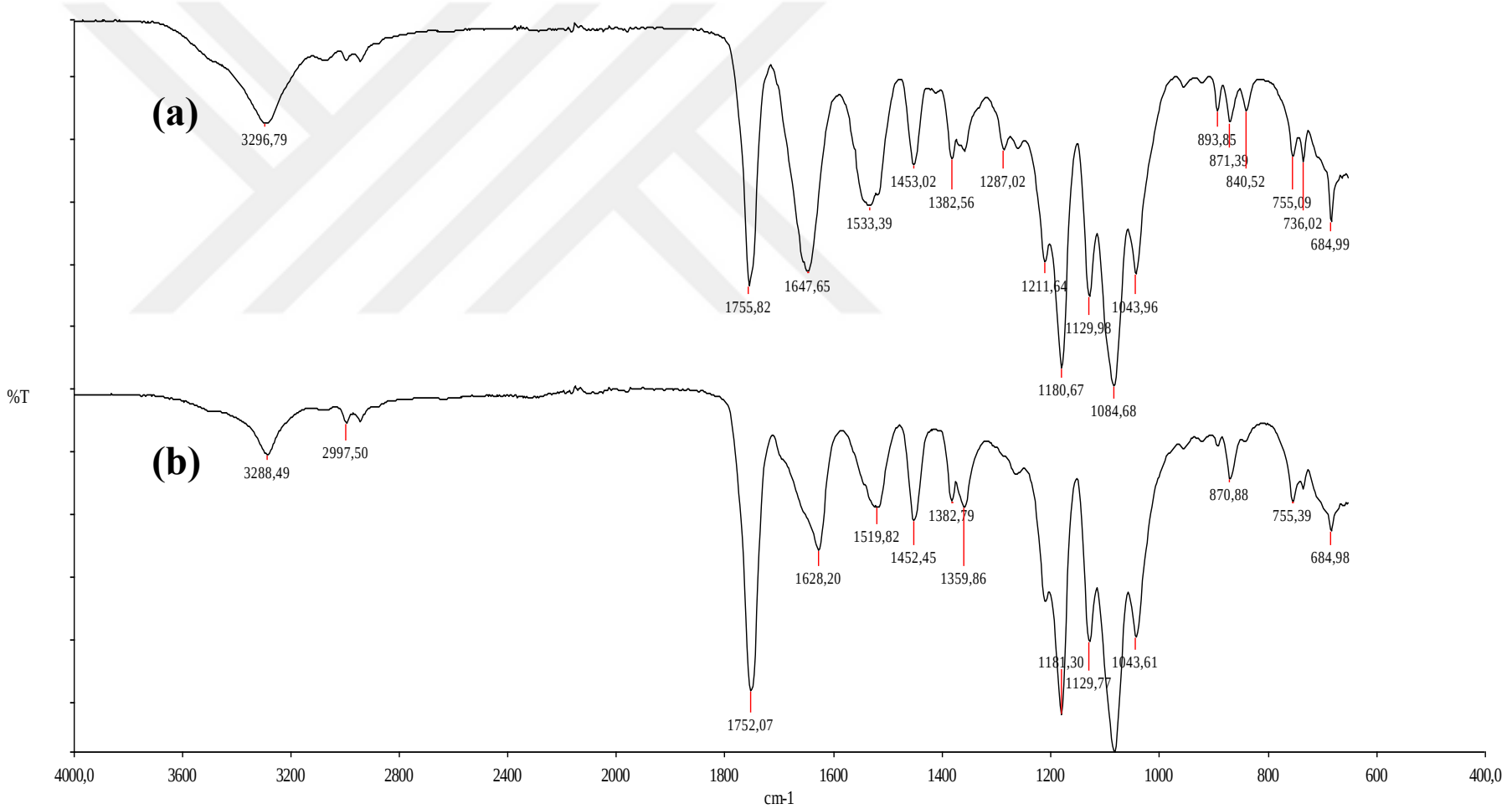

Figure 3.3 : Comperative FTIR spectra of SF:PLLA (1:3 w/w) scaffolds: (a) the scaffold without methanol treatment, whereas (b) the scaffold with methanol treatment.

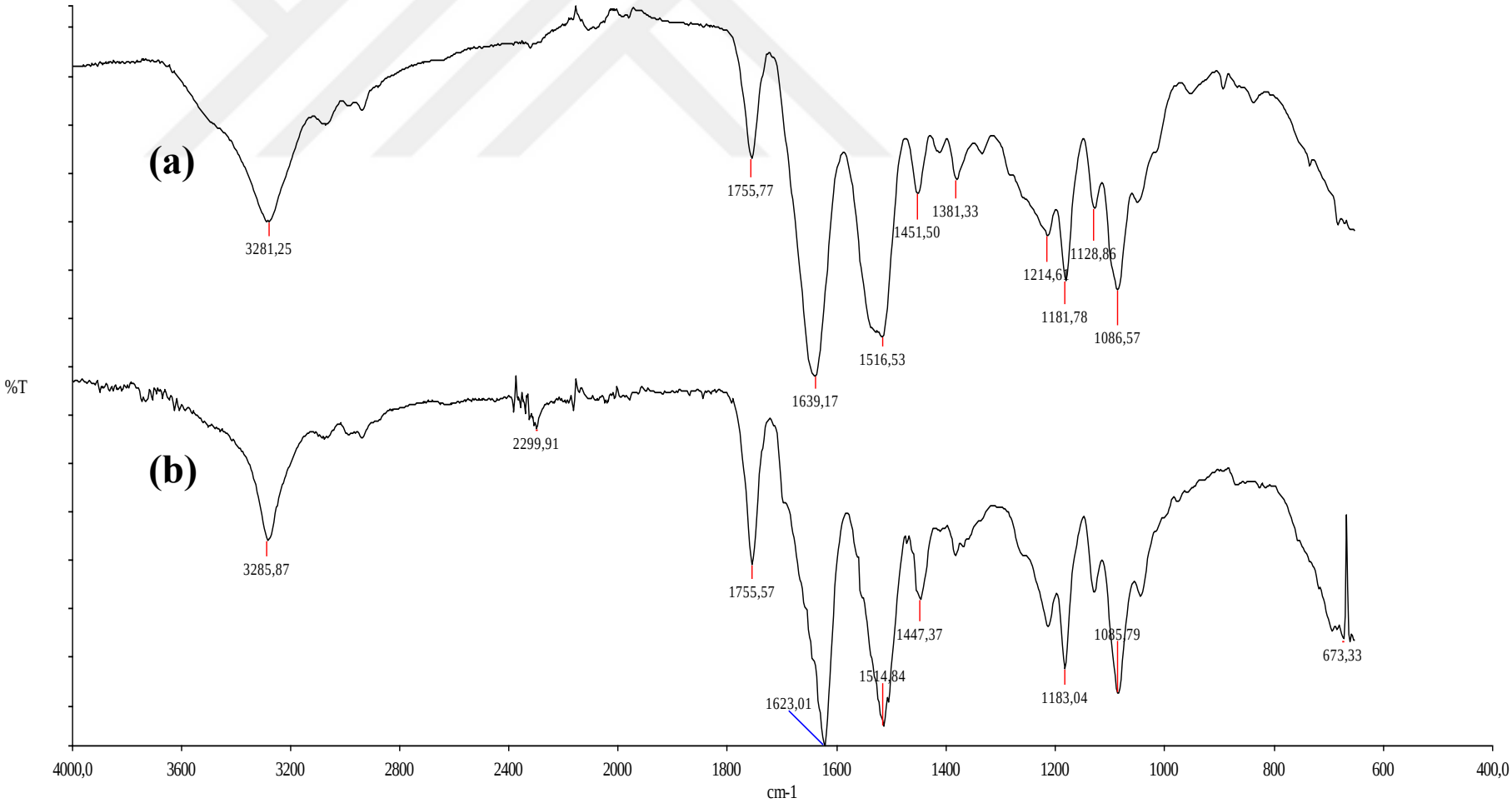

Figure 3.4 : Comperative FTIR spectra of SF:PLLA (3:1 w/w) scaffolds: (a) the scaffold without methanol treatment, whereas (b) the scaffold with methanol treatment.

3.2. Water Uptake Behaviour of Composite Scaffolds

The water uptake ability of scaffolds depends on the polymer composition and hydrophilicity of polymer (Asefnejad et al., 2011). SF:PLLA (1:3 and 3:1 w/w) scaffolds showed different water absorption abilities. The results were obtained for 1 hour and 24 hour for both scaffolds (Figure 3.5).

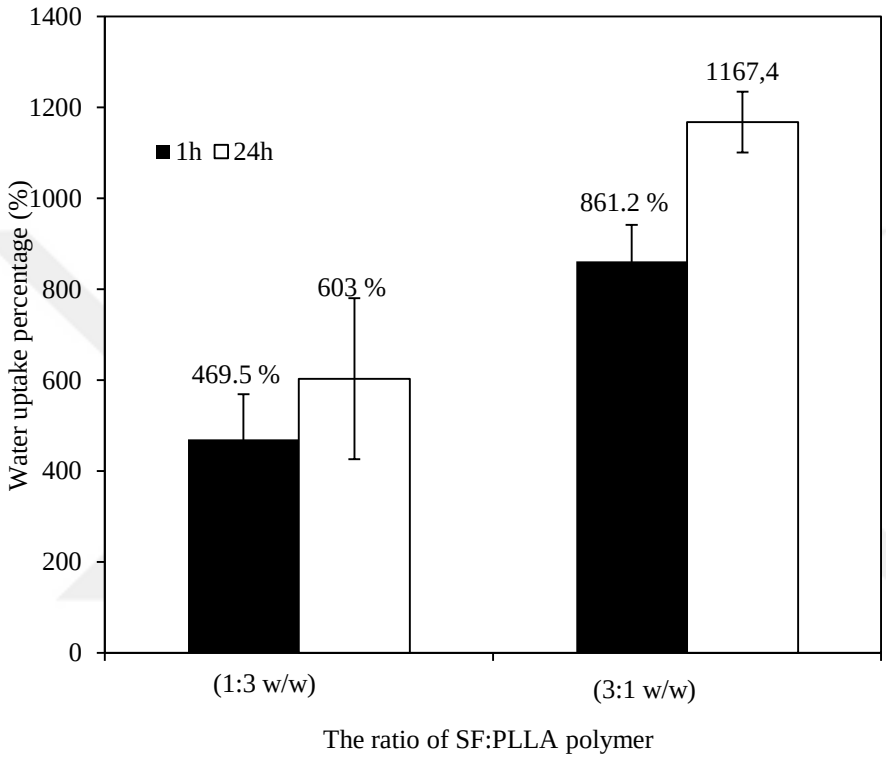

Figure 3.5: Water uptake behaviour of composite scaffolds for 1h and 24h.

Water retention is an important property that has influence the cell seeding and mass transport (Liang et al., 2010). Both scaffolds showed high water uptake capacities (> 400%). The average of water uptake ratios were approximately 469.5% and 861.2% after 1h and 24h, respectively for SF:PLLA (3:1 w/w) scaffolds. On the other hand, the averages were calculated as 603% and 1167.45% after 1h and 24h respectively for SF:PLLA (1:3 w/w). The water uptake ratios showed that increased fibroin concentration in composite scaffolds resulted in higher water absorption. Silk fibroin actually is more hydrophilic than PLLA because of included hydrophilic and hydrophobic amino acid chains (Orue et al., 2016; Mondal et al., 2007). For this reason, fibroin had showed higher water uptake capacity than PLLA polymer.

3.3. Biodegradation Analysis of Composite Scaffolds

Degradation process was carried out on scaffolds with 0.1U/mL concentration of protease XIV enzyme and control (without enzyme) at 37℃ in PBS solution for two months. Generally, PLLA degradation was studied in PBS solution without enzyme (Wojasiński et al., 2013; Wan et al., 2007) since PLLA degraded via hydrolysis, not with enzyme action. For the degradation of silk fibroin, α-chymotrypsin, collagenase IA and protease XIV enzymes are frequently used and it is shown that protease XIV enzyme is significantly effective on fibroin degradation (Li et al., 2003). Sodium azide was used to prevent microbial contamination. Both composite scaffolds showed a steady degradation profile until week 6 (Figure 3.6).

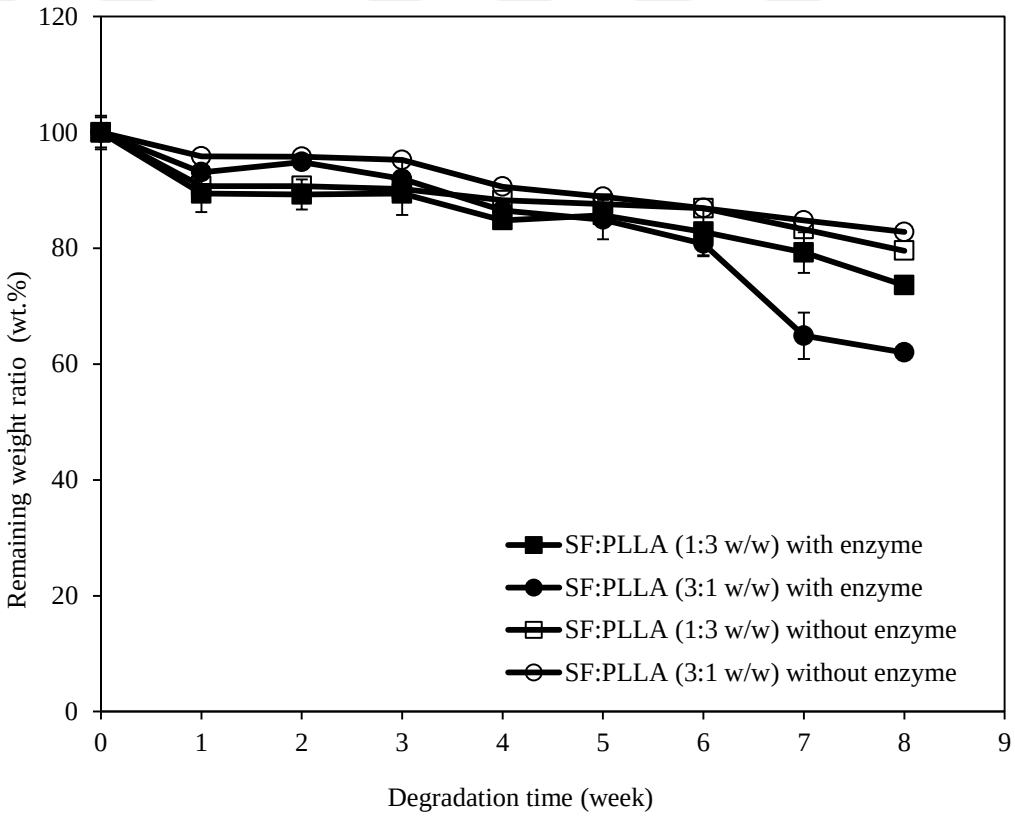

Figure 3.6: Remaining weight ratios of composite scaffolds with and without 0.1U/ml protease XIV enzyme in PBS for two months.

SF:PLLA (3:1 w/w) scaffolds degraded more than SF:PLLA (1:3 w/w) scaffolds in the presence of protease enzyme after two month. The remaning weight ratio values of scaffolds were 73.5% and 61.9% for SF:PLLA (1:3 w/w) and SF:PLLA (3:1 w/w), respectively. During the first 6 weeks, both scaffolds had similar degradation profile but after that, weight loss increased in the high fibroin samples (Figure 3.6).

Eventually, protease enzyme induced the degradation of scaffolds due to silk fibroin presence. However, the weight loss values were 79.5%, 82.8% for SF:PLLA (1:3 w/w) and (3:1 w/w), respectively in the absence of enzyme at the end of 8 week.

In most of the studies, silk fibroin has showed slow degradation than PLLA polymer in tissue engineering (Huang et al., 2007). Silk is slowly adsorbed *in vivo* and degradable over longer period. Degradation rate of fibroin can however be vary when used in different forms (films, foams etc.) for tissue engineering (Liu and Ma, 2004).

3.4. Biomineralization Analysis of Composite Scaffolds

3.4.1. Weight changes of composite scaffolds in mSBF solution during mineralization

Biomineralization process was applied on both OSN-immobilized and without peptides scaffolds with 1x and 3x mSBF concentration for one month. At 1, 3, 7, 14, 21 and 28th day, the weight changes of scaffolds were observed and the effect of peptide on mineralization was examined.

The weights of scaffolds always change during mineralization process. HAp crystals on surfaces induces weight gain in polymer, on the other hand acceralation of polymer degradation causes weight loss in scaffolds (pH change). Some differences in conditions such as pH changes on surface and also the concentrations of copolymers which influence the hydrophilic/hydrophobic properties, affects the weight loss of scaffolds (Liu and Ma, 2004; Wan et al., 2007).

Silk fibroin has higher hydophilicity than PLLA polymer with hydrophilic blocks of amino acids. PLLA has more carboxylic groups to be activated for peptide immobilization by EDC/NHS coupling reaction. It can be presumed that more peptide immobilization occurs on SF:PLLA (1:3 w/w) scaffolds. The degradation of hydrophilic polymers is generally faster than that of hydrophobic polymers (Sung et al., 2004). Rate of degradation can also be modulated with surface modifications or forming composite structures with tunable hydophilic/hydrophobic properties (Lu et al., 2000). Since the degradation and mineralization took place at the same time, it is hard to differentiate the degree of mineralization from the weight gain in scaffolds and fluctuating curves were obtained (Figure 3.7 and Figure 3.8). Solution with lower ion concentration (1xmSBF) seemed to result in an apparent weigth gain in

scaffolds whereas the less weight gain and weight loss at 3xmSBF sample. High ionic concentration might have caused an accelerated weight loss on scaffolds. Briefly, the effect of OSN peptides could not be clearly observed form weight changes of scaffolds.

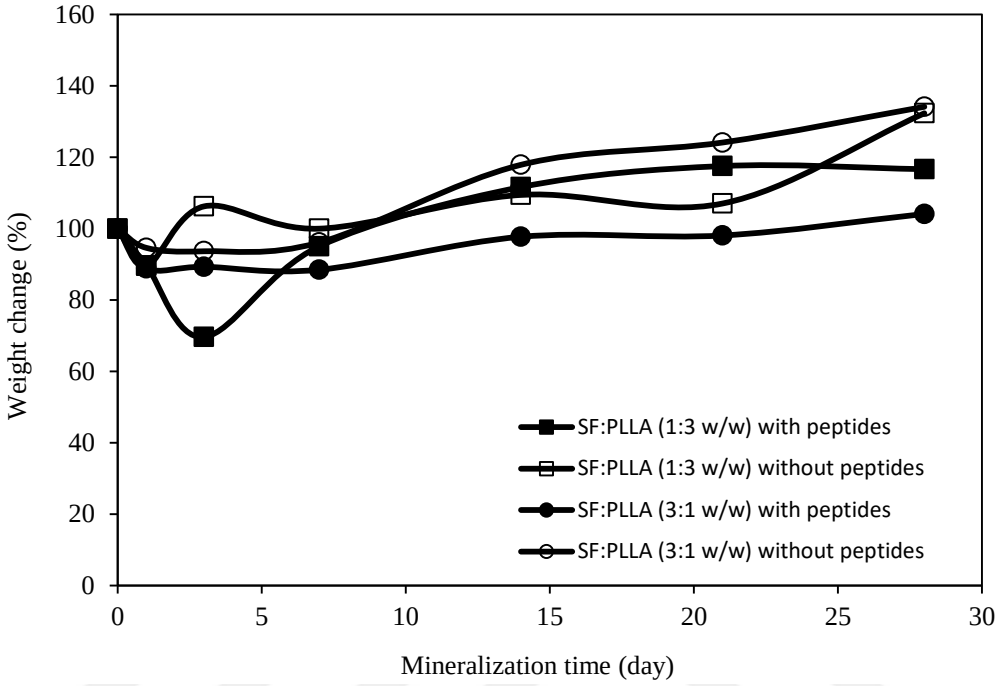

Figure 3.7: The weight changes of composite scaffolds with OSN peptides and without peptides in 1xmSBF solution for a month.

The SF:PLLA (1:3 w/w) scaffolds with and without peptides showed 16.66% and 32.32% weight gain, respectively with 1xmSBF (Figure 3.7) and these scaffolds with and without peptides showed 12% and 4.55% weight loss, respectively with 3xmSBF (Figure 3.8). On the other hand, The SF:PLLA (3:1 w/w) scaffolds showed 4.12% and 34.14% weight gain for OSN-immobilized and without peptides forms, respectively with 1xmSBF (Figure 3.7) and these scaffolds showed 3% and 6.31% weight gain for both OSN-immobilized and without peptides forms with 3xmSBF (Figure 3.8).

The scaffolds, which were incubated in 1xmSBF solution for a month, showed weight gain. On the other hand, the scaffolds, which were incubated in 3xmSBF solution showed less weight gain and weight loss on both polymer scaffolds. The more weight changes were observed for scaffolds that incubated 3xmSBF solution during mineralization process.

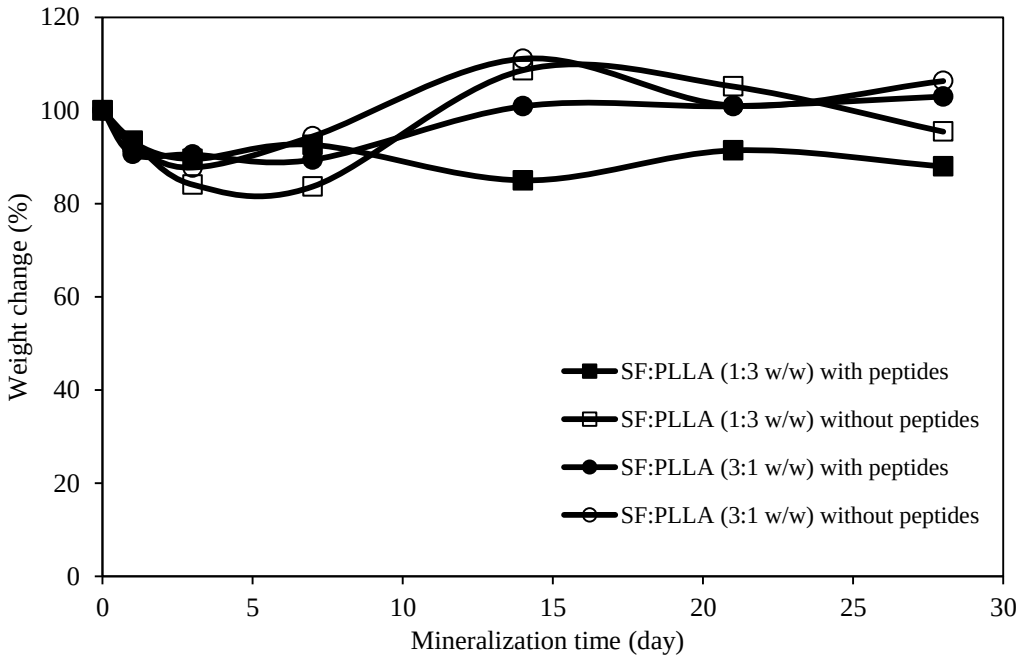

Figure 3.8: The weight changes of composite scaffolds with OSN peptides and without peptides in 3xmSBF solution for a month.

OSN peptide chain induces the rate of mineralization on stainless steel surfaces from amorphous calcium phophates to HAp crystals as adopted from Hosseini *et al*. (Hosseini et al., 2014). OSN peptide can increase hydrophilicity of scaffolds and affected aggregated ion concentration on polymer surfaces in mSBF solution. In particular, the degradation product of PLLA polymer causes acidification of local environment and accelerates degradation (Martin et al., 1996). However, weight increases of scaffolds should occur by HAp crystal growth in both mSBF solutions. However, the SF:PLLA (1:3 w/w) scaffolds had weight losses at the end of process because of faster degradation rate with higher ion concentration in 3xmSBF.

3.4.2. SEM images and EDS results of mineralized scaffolds after mineralization

After mineralization process, the morphologies of scaffolds that mineralized within 1xmSBF and 3xmSBF solution were investigated with SEM after 2, 3 and 4 week of mineralization. Additionally, EDS analysis were carried out for scaffolds in 1xmSBF solution. During EDS analysis, the deformation occured on surfaces of polymer scaffolds that incubated with 3xmSBF solution. SEM images of scaffolds were investigated for both mSBF concentration for 2, 3 and 4 weeks after mineralization (Figure 3.9 and Figure 3.10).

OSN-immobilized and without peptide forms of SF:PLLA (1:3 w/w) scaffolds were investigated after 2, 3 and 4 week of mineralization with 1xmSBF (Figure 3.9).

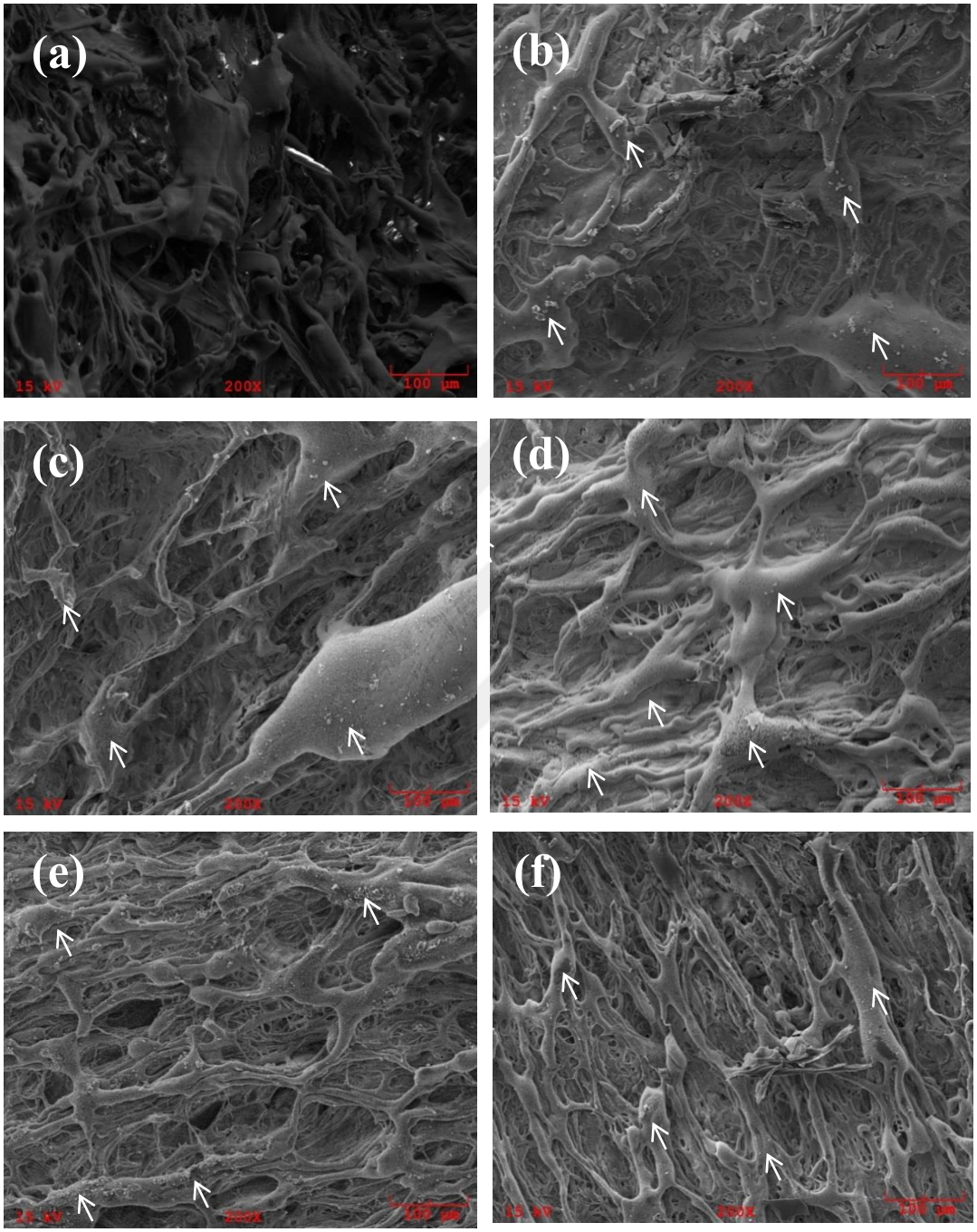

Figure 3.9: SEM images of SF:PLLA (1:3 w/w) scaffolds; (a), (c) and (e) without peptide, after 2, 3 and 4 week of mineralization; (b), (d) and (f) with peptide after 2, 3 and 4 week of mineralization with 1xmSBF. Arrows show the minerals.

Minerals were observed in all samples but after 2nd week of mineralization, lower mineralized area was observed onto scaffold without peptides (a). On the other hand, after 3rd week of incubation, both scaffolds showed higher mineralized area on the

surfaces of polymers. The SF:PLLA (3:1 w/w) scaffolds were analyzed after 2, 3 and 4 week of mineralization with 1xmSBF solution (Figure 3.10).

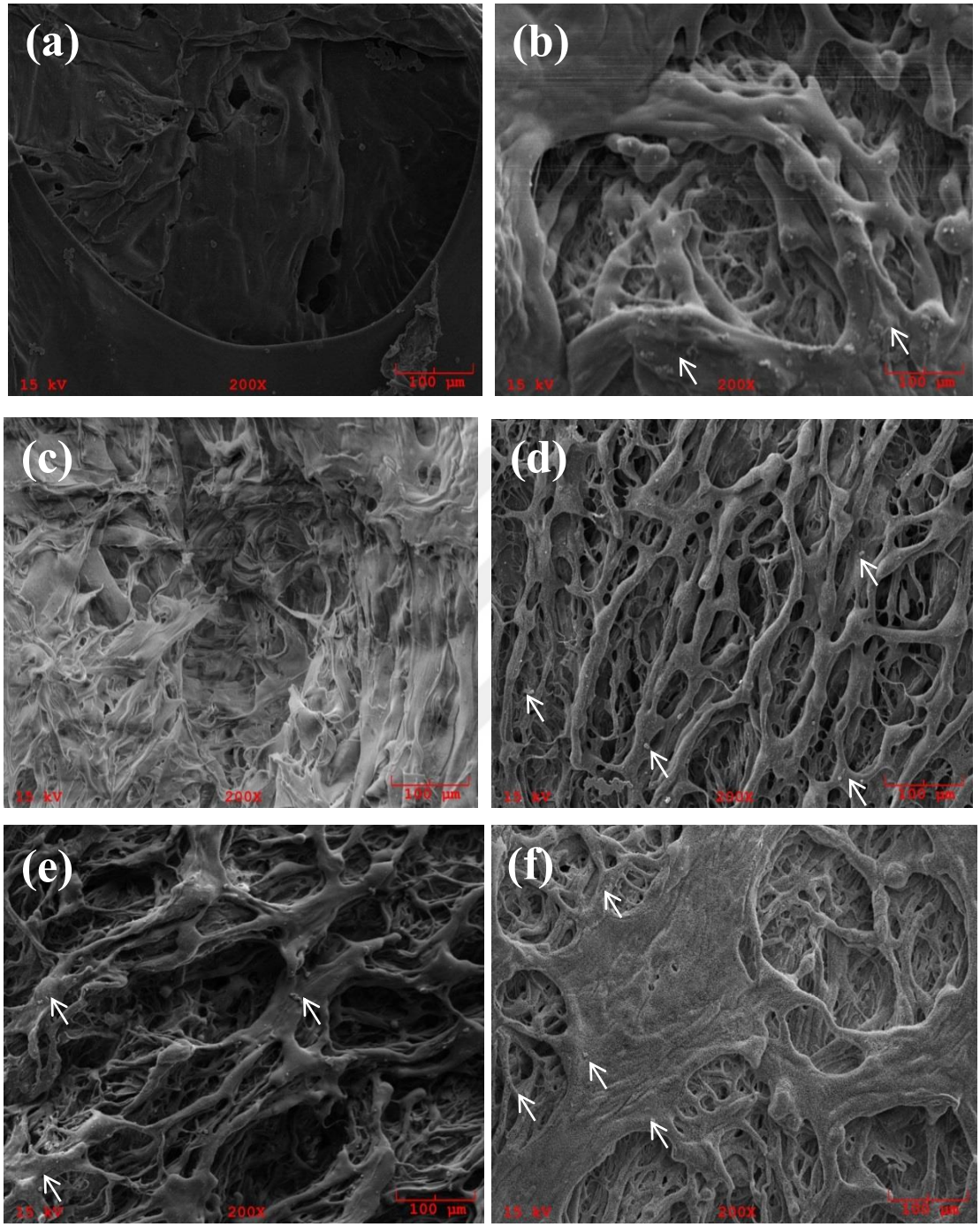

Figure 3.10: SEM images of SF:PLLA (3:1 w/w) scaffolds; (a), (c) and (e) without peptides after 2, 3 and 4 week of mineralization; (b), (d) and (f) with peptides after 2, 3 and 4 week of mineralization in 1xmSBF. Arrows show the minerals.

The higher calcium accumulation was observed on the surfaces of OSN-immobilized scaffolds especially after 3 and 4 week of mineralization. According to the images, the SF:PLLA (1:3 w/w) scaffolds without peptides showed expand mineralized area on the surfaces from 3rd week than SF:PLLA (3:1 w/w) scaffolds without peptide

because of the presence of more carboxylic acid residues in SF:PLLA (1:3 w/w) scaffolds. On the other hand, both OSN-immobilized SF:PLLA (1:3 w/w) and SF:PLLA (3:1 w/w) scaffolds showed expand mineralized and calcified areas on the surfaces of polymers that began from 2nd week of incubation. It seemed that presence of OSN peptide had a positive effect on mineralization on both structures but the effect was not very pronounced. OSN peptides are HAp binding peptides and they have an effect on crystallization of HAp (Hosseini et al., 2013), so the crystal structure of minerals should also be determined to have more detailed information on peptide usage. The Ca/P atomic ratios of scaffolds were calculated for SF:PLLA (1:3 w/w) and SF:PLLA (3:1 w/w) scaffolds.

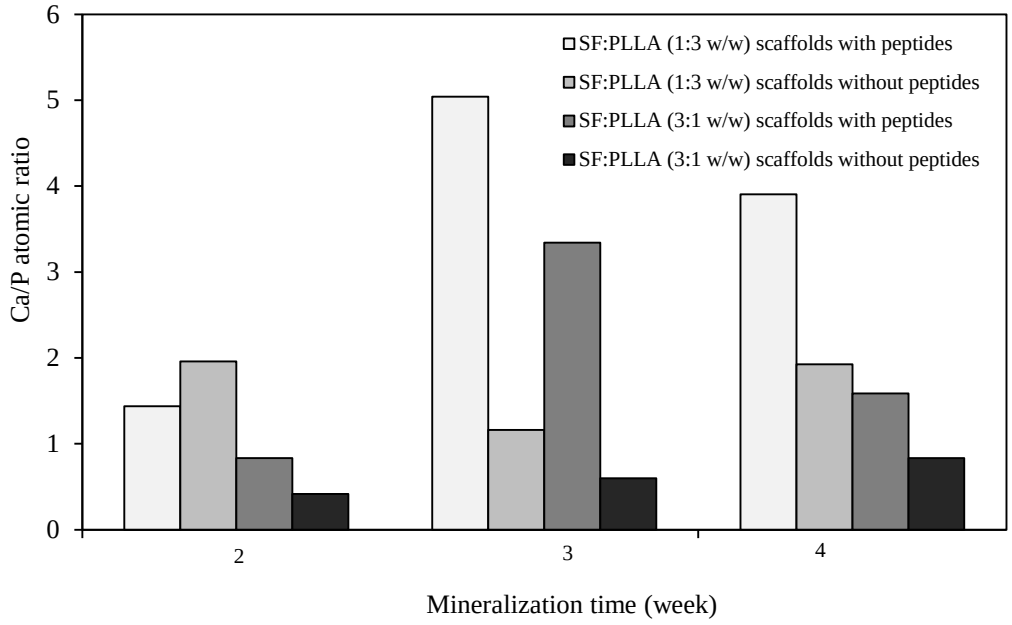

Figure 3.11: The Ca/P atomic ratio (%) of SF:PLLA (1:3 w/w) and SF:PLLA (3:1 w/w) scaffolds with and without peptides in 1xmSBF solution.

As shown above, the Ca/P atomic ratios of SF:PLLA (1:3 w/w) scaffolds with peptides were 5.04 and 3.90 after 3 and 4th week, respectively. On the other hand these Ca/P atomic ratios were found to be as 1.16 and 1.92 for SF:PLLA (1:3 w/w) without peptides after 3 and 4th week, respectively. Lastly, SF:PLLA (3:1 w/w) scaffolds with peptides had 3.34 and 1.58 Ca/P atomic ratios after 3 and 4th week, respectively. The Ca/P ratios of SF:PLLA (3:1 w/w) scaffolds with peptides after 4th week of mineralization and SF:PLLA (1:3 w/w) scaffolds with peptides after 2nd week of mineralization were 1.58 and 1.43 respectively and closed to the stoichiometric value of HAp (1.67). The scaffolds which had higher amount of calcium and lower amount of phosphorus than HAp, showed calcified surfaces

because of the more calcium accumulation. The morphologies of both SF:PLLA (1:3 w/w) and SF:PLLA (3:1 w/w) scaffolds with and without peptides after 2, 3 and 4 week of mineralization with 3xmSBF solution were also analyzed with SEM.

It was presumed that the scaffolds, which incubated within 3xmSBF, had more minerilized and calcified areas than the scaffolds incubated in 1xmSBF solution. HAp minerals in few scaffolds could easily be detected until 4 weeks in 3xmSBF for scaffolds with peptides (Figure 3.12 and Figure 3.13).

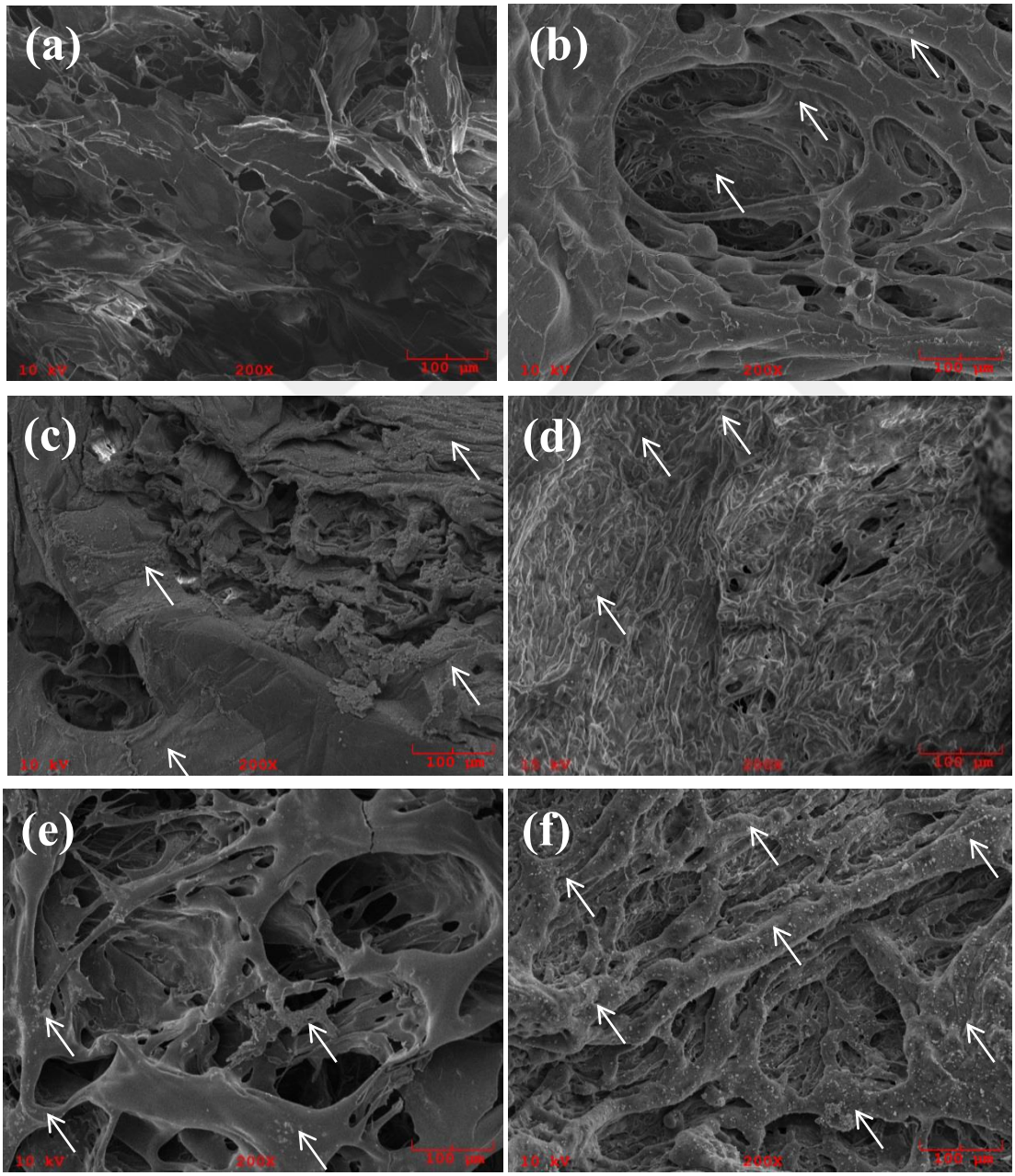

Figure 3.12: SEM images of SF:PLLA (1:3 w/w) w/v scaffolds; (a), (c) and (d) without peptide after 2, 3 and 4 week mineralization; (b), (d) and (f) with peptide after 2, 3 and 4 week mineralization with 3xmSBF. Arrows show the minerals.

Additionally, it was observed that porosities in all scaffolds provided spaces for the penetration of calcium and phosphates ions from mSBF solution so minerals could also be detected inside these pores (data not shown).

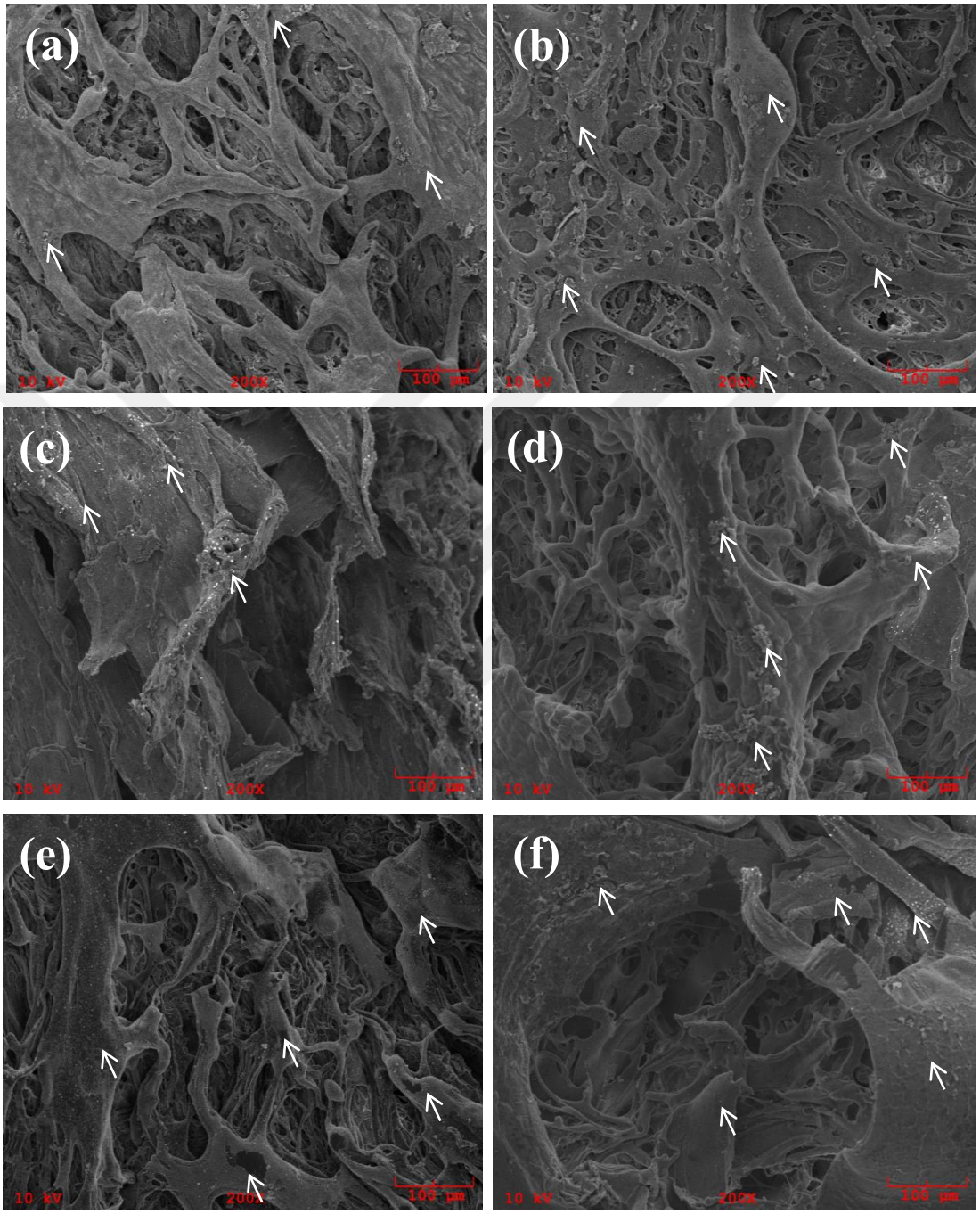

Figure 3.13: SEM images of SF:PLLA (3:1 w/w) w/v scaffolds; (a), (c) and (e) without peptide after 2, 3 and 4 week mineralization; (b), (d) and (f) with peptide after 2, 3 and 4 week mineralization with 3xmSBF. Arrows show the minerals.

3.4.3. FTIR spectrum of mineralized scaffolds

To examine the HAp crystal growth on scaffolds, FTIR spectrum were investigated for both scaffolds at different time intervals (1, 3, 7, 14, 21 and 28th day). The absorption bands of composite scaffolds were analyzed and classified as PLLA, silk fibroin and HAp crystal bands and shown in Table 3.1 for SF:PLLA (1:3 w/w) and in Table 3.2 for SF:PLLA (3:1 w/w) scaffolds. The scaffolds without peptide were analyzed only for 3xmSBF samples. The peaks of PLLA chemical groups are abundant and strong and it made difficult to distinguish between PLLA and hydroxyapatite groups. It was presumed that some chemical groups overlapped.

The characteristic bands of HAp occurs with CO_3^{2-}, PO_4^{3-} and OH^- chemical groups (HAp analysis) and according to the results, hydroxyapatite formation started at the end of 1st week and continued during 4 week of mineralization. The FTIR absorption bands of SF:PLLA (1:3 w/w) scaffolds before mineralization and during 4 weeks of mineralization were shown in Table 3.1 and Figure 3.14.

Table 3.1: FTIR absorption bands of SF:PLLA (1:3 w/w) scaffold during mineralization for 28 days.

	Scaffolds before mineralization and after 1st, 3th, and 7th days of mineralization with 3xmSBF		After 14st, 21th, and 28th days of mineralization wth 3xmSBF	
Component	Absorption bands (cm^{-1})	Chemical groups	Absorption bands (cm^{-1})	Chemical groups
PLLA	Around 3286 (Dopfer et al., 2002)	CH_2 bending	Around 3286 (Dopfer et al., 2002)	CH_2 bending
	2997.29 (Krikorian and Pochan, 2005)	CH_3 asymmetric stretching	2997.68 (Krikorian and Pochan, 2005)	CH_3 asymmetric stretch
			Around 1755 (Al-Jallad et a., 2014)	C=O carbonyl stretching
	Around 1750 (Fakirov, 2015)	C=O carbonyl stretching	Around 1750 (Fakirov, 2015)	C=O carbonyl stretching
	1751.94 (Hawari et al., 2014)	-C=O stretching	1453.15 (Boccaccini, 2007)	CH_3 asymmetric bend
	Around 1451-1452 (Fang et al., 2009; Ceyhan et al., 2008)	-CH(CH_3)	1452 (Fang et al., 2009)	-CH(CH_3)

Table 3.1 (continued): FTIR absorption bands of SF:PLLA (1:3 w/w) scaffold during mineralization for 28 days.

	Scaffolds before mineralization and after 1st, 3th, and 7th days of mineralization with 3xmSBF		After 14st, 21th, and 28th days of mineralization wth 3xmSBF	
Component	Absorption bands (cm^{-1})	Chemical groups	Absorption bands (cm^{-1})	Chemical groups
PLLA	1383-1384 (Kim et al., 2008)	CH_3 asymmetric bending	1358-1359 (Ge et al., 2014)	-CH- asymmetric bending
	1358 -1359 (Ge et al., 2014)	-CH- asymmetric bending	Around 1181-1182 (Lu et al., 2011)	C-O-C stretching
	Around 1181 (Lu et al., 2011)	C-O-C stretching	1130,04 (Sobczak et al., 2008)	C-O stretching
	Around 1129 (Zimmermann et al., 2013)	C-C-O stretching	Around 1127 (Mohanty et al., 2015)	-C-O stretching
	1083, 33 (Hawari et al., 2014)	-C-O-	Around 1082 (Sobczak et al., 2008)	C-O stretching
	Around 1081 (Ninaya et al., 2016)	$-CH_3$ stretching	1042-1043 (Krikorian and Pochan, 2005)	- $C-CH_3$ stretching
	1042-1043 (Krikorian and Pochan, 2005)	$-C-CH_3$ stretching		
	Around 869 (Emiliani et al., 2015)	C-C stretching		
	756.21 (Nogueira et al., 2015)	CH_2 stretching		
SF	Around 3286 (Eslahi et al., 2014)	N-H stretching	3285.35 (Tunma et al., 2013)	N-H stretching
	1622-1627 (Hu et al., 2006)	C=O stretching vibrations of the peptide bonds (beta sheet)	1622-1627 (Hu et al., 2006)	C=O stretching vibrations of the peptide bonds (beta sheet)
			Around 1523.13 (Monti et al., 2007)	N-H stretching (amide II)
			Around 1526-1528.16 (Barth, 2007)	N-H stretching (amide II) beta sheet structure

Table 3.1 (continued): FTIR absorption bands of SF:PLLA (1:3 w/w) scaffold during mineralization for 28 days.

	Scaffolds before mineralization and after 1st, 3th, and 7th days of mineralization with 3xmSBF		After 14st, 21th, and 28th days of mineralization wth 3xmSBF	
Component	Absorption bands (cm^{-1})	Chemical groups	Absorption bands (cm^{-1})	Chemical groups
SF	Between 684-694 (Tho et al., 2013)	N-H wag of 1^o, 2^o amines	Around 1210 (Lu et al., 2011) Between 684-694 (Tho et al., 2013)	N-H stretching amide III N-H wag of 1^o, 2^o amines
	2345.68 (Innes et al., 2007)	due to CO_2 in the air	Around 3288.30 (Prabu S et al., 2014) 3374.47 (Meejoo et al., 2006)	OH^- group Adsorbed water
HAp Crystal	1039.83 (Venkatasubbu et al., 2011)	P-O stretching	Around 1035 (Barros et al., 2016) Around 871 (Figueiredo et al., 2012)	PO_4^{3-} stretching CO_3^{2-} stretching

The absorption bands of PLLA polymer are the ones for CH_2, CH_3 stretching, C-C, C-H, C-O-C, C-C-O, C-O, -C-CH_3, CH (CH_3) stretching, C=O stretching groups especially intensed between 756-1755 cm^{-1} wavelenghts for SF:PLLA (1:3 w/w) scaffolds. These absorption bands belongs to characteristic groups of PLLA polymers. The chemical groups of silk fibroin was obtained between 684-1627 cm^{-1} for N-H stretching, amide II and amide III in beta sheet forms and C=O stretching of peptide bonds. The characteristic peaks of fibroin in Amide I region could not be clearly observed because of PLLA groups.

The absorption peak at 1039.38 cm^{-1} showed P-O stretching, which belongs to HAp crysal after 1st week of incubation for SF:PLLA scaffolds. The absorption peaks at 871.26 and 871.18 cm^{-1} showed presence of carbonate (CO_3^{2-}) groups which belongs to hydroxyapatite crystals after 3 and 4th week of incubation. The absorption peak at 1035.61 showed PO_4^{-3} groups of HAp. Additionally, the peaks at 3374 and 3288 cm^{-1} showed the presence of absorbed water and OH^- groups which is characteristic group of HAp after 1 week of mineralization (Figure 3.14).

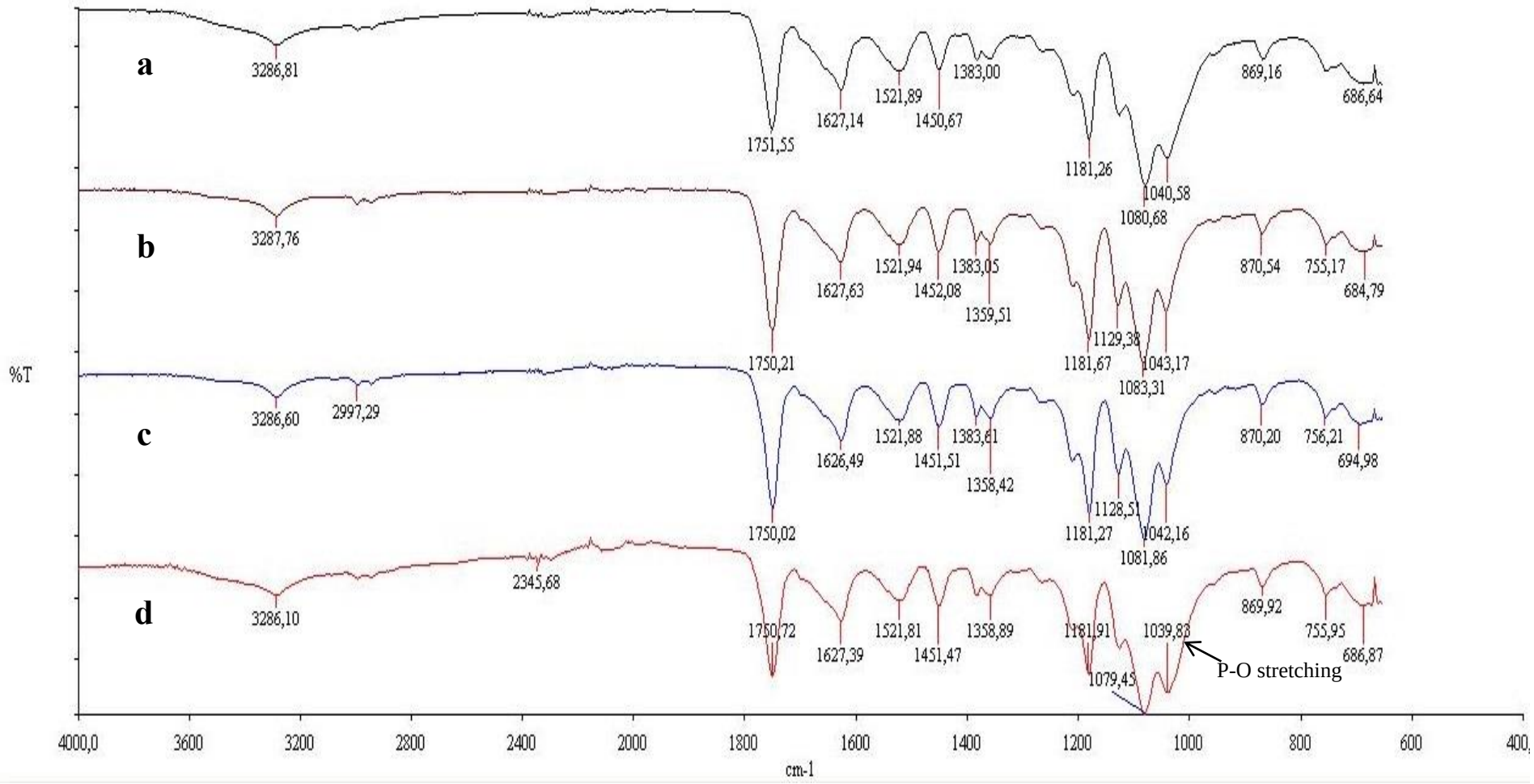

Figure 3.14: FTIR spectra of SF:PLLA (1:3 w/w) samples; before mineralization (a); after the 1st (b), 3th (c) and 7th(d) days of mineralization process with 3xmSBF.

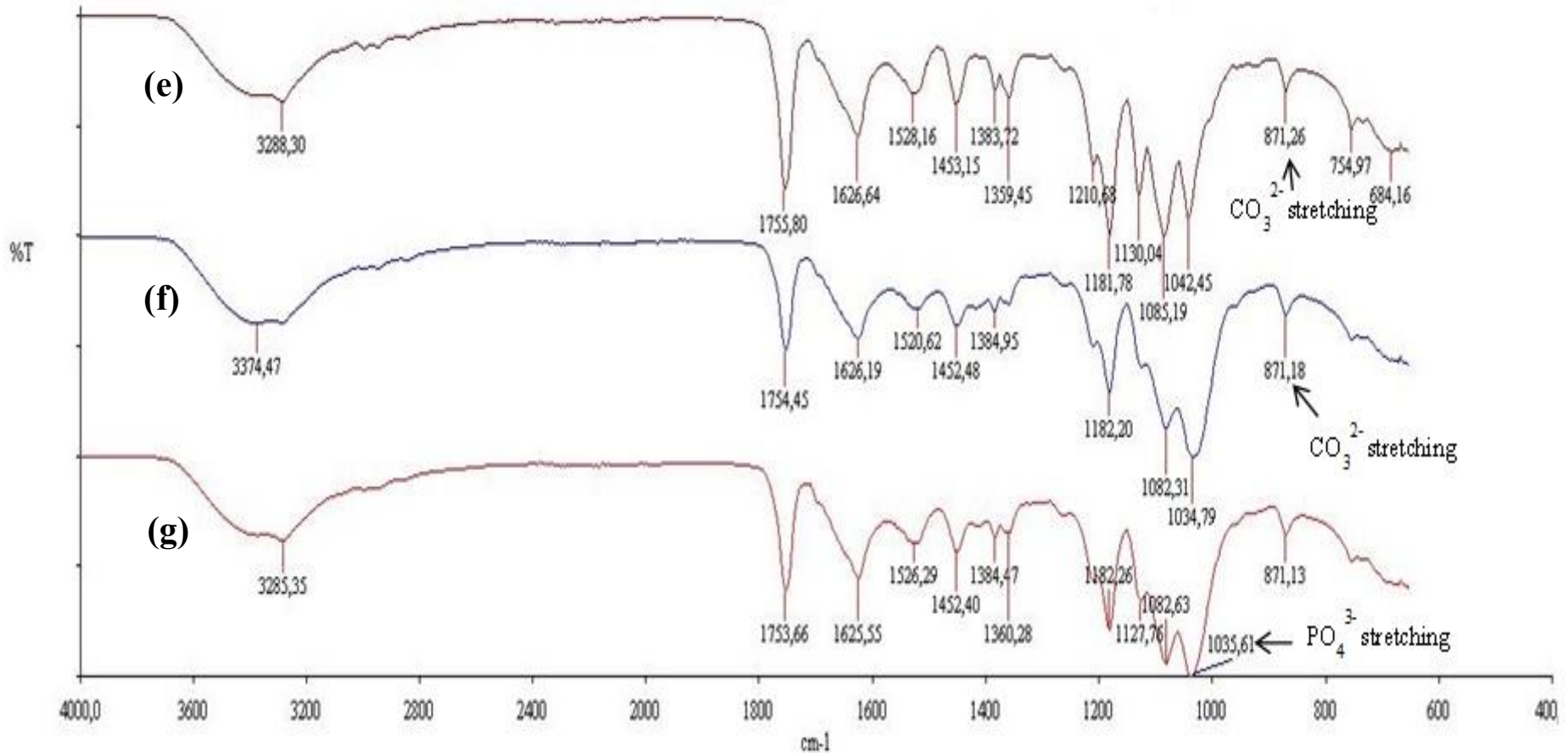

Figure 3.14 (continued): FTIR spectrum of SF:PLLA (1:3 w/w) samples after the 14th (e), 21th (f) and 28th (g) days of mineralization with 3xmSBF.

The FTIR results of SF:PLLA (3:1 w/w) scaffolds before mineralization and for a month of mineralization were shown in Table 3.2. The absorption bands of PLLA showed up between 1042-1755 cm^{-1} wavelenghts for C=O stretching, CH_3, C-C-O, C-O-C and –C-CH_3 chemical groups. The chemical groups of fibroin was obtained especially between 684-1627 cm^{-1} wavelenghts for N-H stretching of 1^o and 2^o amines and C-N stretching of aliphatic amine and C=O stretching of peptide bonds.

Table 3.2: FTIR absorption bands of SF:PLLA (3:1 w/w) scaffold during mineralization for 28 days.

	Scaffolds before mineralization and after 1^{st}, 3^{th}, and 7^{th} days of mineralization with 3xmSBF		After 14^{st}, 21^{th}, and 28^{th} days of mineralization with 3xmSBF	
Component	Absorption bands (cm^{-1})	Chemical groups	Absorption bands (cm^{-1})	Chemical groups
PLLA	Around 1755 (Al-Jallad et a., 2014)	C=O carbonyl stretching	Around 1755 (3 Al-Jallad et a., 2014)	C=O carbonyl stretching
	1383-1384 (Kim et al., 2008)	CH_3 bending	1181-1182 (Lu et al., 2011)	C-O-C stretching
	1130,04 (Sobczak et al., 2008)	C-O stretching	1130.04 (Sobczak et al., 2008)	C-O stretching
	Around 1129 (Zimmermann et al., 2013)	C-C-O stretching	Around 1085-1086 (Shi et al., 2016)	-C-O-C-
	1085-1086 (Shi et al., 2016)	-C-O-C-		
	Between 1042-1044 (Krikorian and Pochan, 2005)	-C-CH_3 stretching		
SF	3285,35 (Georgieva et al., 2001)	N-H stretching	1622-1627 (Hu et al., 2006)	C=O stretching of the peptide bonds (beta sheet)
	1622-1627 (Hu et al., 2006)	C=O stretching of the peptide bonds (beta sheet)		
	Around 1514 (Zhang et al., 2012)	N-H stretching (amide II) beta sheet structure	Around 1514 (Zhang et al., 2012)	N-H stretching (amide II) beta sheet structure
	Around 1446-1447 (Barth, 2000)	CH_2 banding of amino acids in fibroin Gly)	Around 1446-1447 (Barth, 2000)	CH_2 banding of amino acids in fibroin(Gly)

Table 3.2 (continued): FTIR absorption bands of SF:PLLA (3:1 w/w) scaffold during mineralization for 28 days.

	Scaffolds before mineralization and after 1st, 3th, and 7th days of mineralization with 3xmSBF		After 14st, 21th, and 28th days of mineralization with 3xmSBF	
Component	Absorption bands (cm^{-1})	Chemical groups	Absorption bands (cm^{-1})	Chemical groups
SF	Around 1214-1213 (Sharma, 2000)	C-N stretching alphatic amine	Around 1214-1213 (Sharma, 2000)	C-N stretching alphatic amine
	Between 684-694 (Tho et al., 2013)	N-H wag of 1^o, 2^o amines	Between 684-694(Tho et al., 2013)	N-H wag of 1^o, 2^o amines
	Between 684-694 (Tho et al., 2013)	N-H wag of 1^o, 2^o amines	Between 684-694 (Tho et al., 2013)	N-H wag of 1^o, 2^o amines
HAp crystal	Around 3281-3282 (Meejoo et al., 2006)	OH^- group	1507.98 (Fleet et a., 2004)	type A carbonate (CO_3HAp)
			1412.06 (Schulte, 2003)	type B carbonate (CO_3HAp)
			Around 1030 (Spevak et al., 2013)	PO_4^{3-} stretching
			1024.65 (Sallam et al., 2012)	PO_4^{3-} stretching
			Around 871 (Figueiredo et al., 2012)	CO_3^{2-} stretching

The HAp formation on SF:PLLA (3:1 w/w) was observed for a month mineralization (Figure 3.15). It was assumed that the absorption band at around 3281 cm^{-1} represented OH^- groups of apatite crystals and the peaks at 1507 and 1412 cm^{-1} showed the presence of type A and B carbonate groups, respectively after 3 weeks of mineralization (Figure 3.15). If the incorporation of carbonate ions occurs in OH^- sublattice, it is named A-type carbonate apatite. If it occurs via PO_4^{3-} displacement, it is named B-type carbonate apatite (Schulte, 2003). The PO_4^{3-} groups appeared at 1030 and 1024 cm^{-1} wavelenghts and the CO_3^{2-} groups of HAp crystals at around 871 cm^{-1} wavelenght 21 and 28th day of incubation.

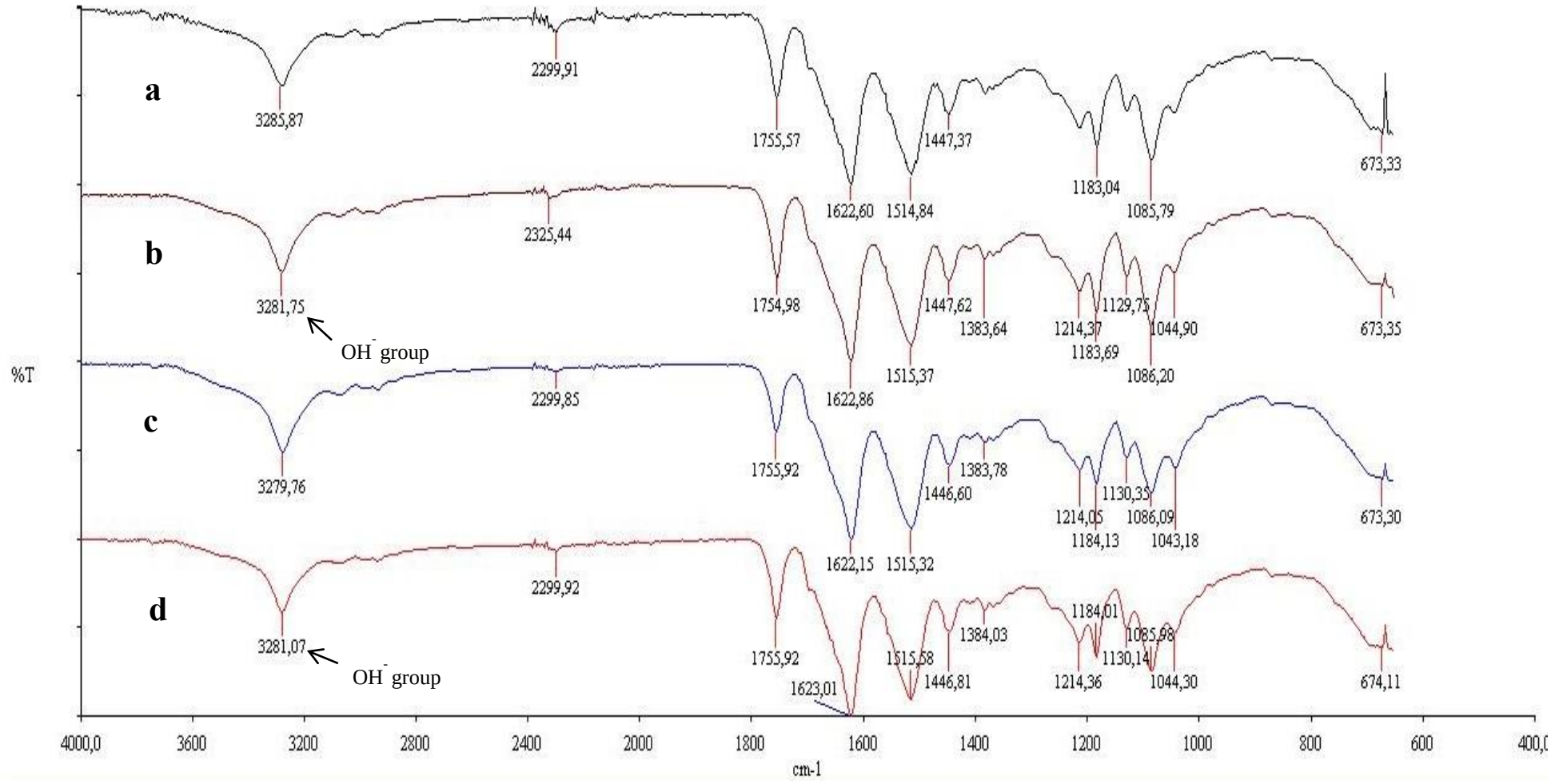

Figure 3.15: FTIR spectrum of SF:PLLA (3:1 w/w) samples; before mineralization (a); after the 1st (b), 3th (c) and 7th(d) days of mineralization process with 3xmSBF.

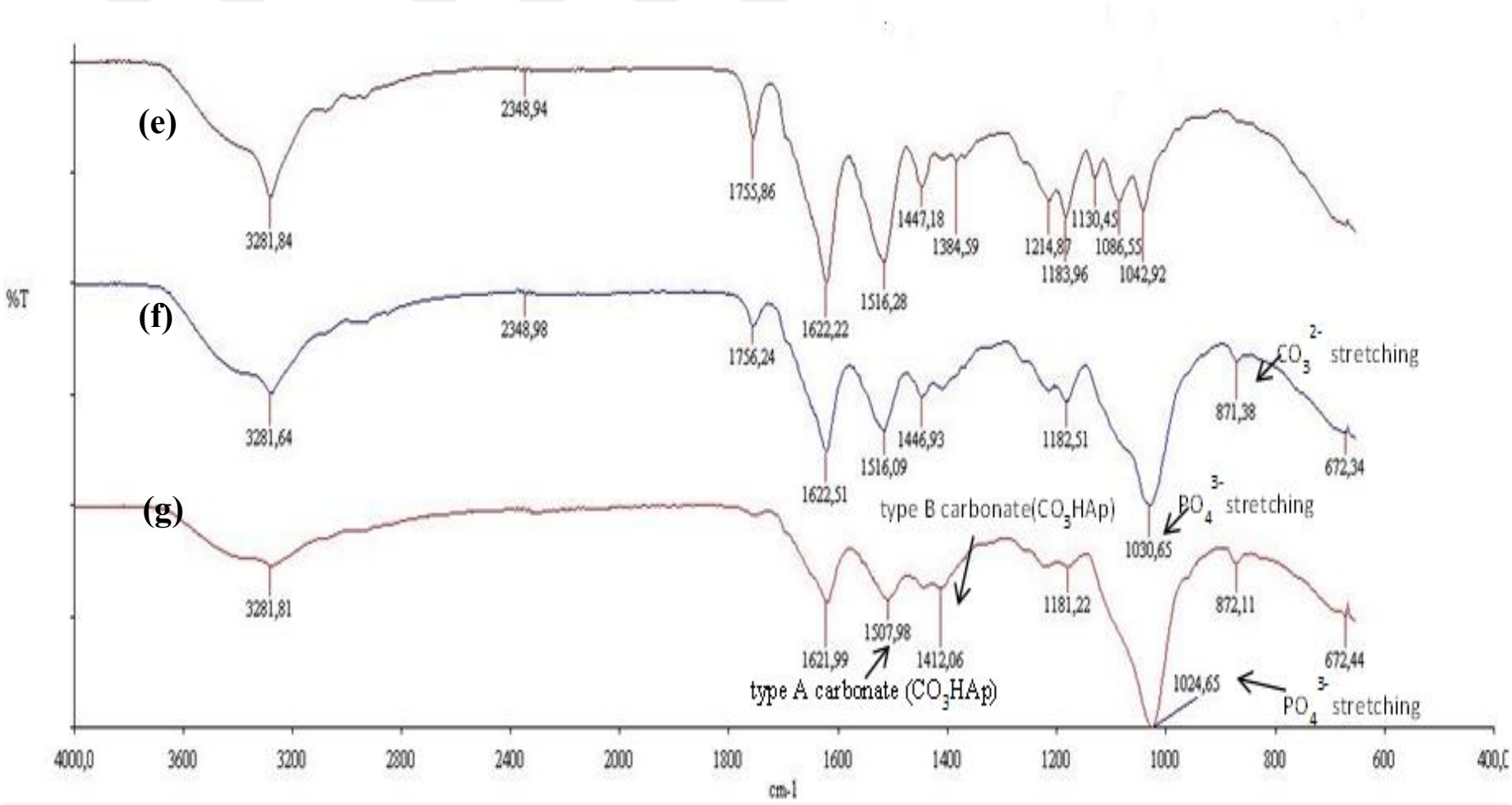

Figure 3.15 (continued): FTIR spectrum of SF:PLLA (3:1 w/w) samples after the 14th (e), 21th (f) and 28th (g) days of mineralization with 3xmSBF.

3.5 Cell proliferation on Composite Scaffolds

The attachment and proliferation of hFOB cells on both scaffolds were investigated via MTS cell proliferation analysis. The number of cells that seeded onto scaffolds before incubation was 20000 and the number of viable cells were calculated at different time intervals of 1, 4 and 7th days with three control samples (Figure 3.16).

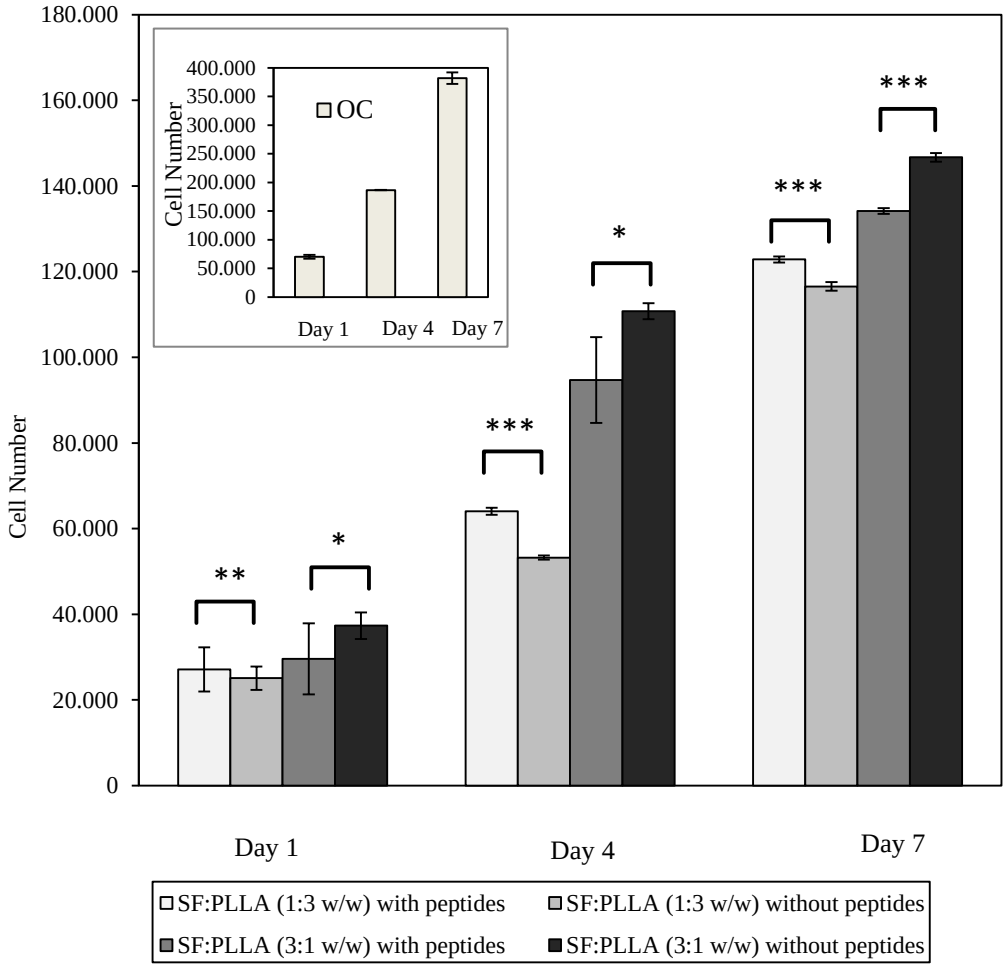

Figure 3.16: Cell numbers of all scaffolds after 1, 4 and 7th day of incubation. (mean±SD, n=3, *$p\leq0.5$, **$p\leq0.1$, ***$p\leq0.05$)

According to these results, SF:PLLA (3.1 w/w) scaffolds had higher cell numbers than SF:PLLA (1:3 w/w) scaffolds especially on 4th day. In their classes, the OSN-immobilized SF:PLLA (1:3 w/w) scaffolds showed higher cell numbers than scaffolds without peptides. But OSN-immobilized SF:PLLA (3:1 w/w) scaffolds had lower cell numbers than scaffolds without peptides. OSN peptides induces cell attachment in stainless steel, as adopted from Hosseini et. al (2013). It was observed that positive effect of peptides on cell proliferation could be seen for SF:PLLA (1:3 w/w) scaffolds while for SF:PLLA (3:1 w/w) scaffolds an opposite trend was seen.

4. CONCLUSIONS AND RECOMMENDATIONS

Bone tissue engineering aims to generate scaffolds to successfully assist bone regeneration with essential properties. The aim of this study was produce composite polymeric scaffolds functionalized with peptides to induce mineralization for rapid improvement. For this, silk fibroin and PLLA were chosen as biomaterials. Fibroin proteins were extracted from the silkworm cocoons and composited with PLLA polymers in two different concentrations as SF:PLLA (1:3 w/w) and (3:1 w/w). The methanol treatment was applied to form insoluble structures with the induction of beta sheets from random coil structures. The OSN peptides were immobilized on polymer surfaces of both composite scaffolds via EDC/NHS coupling reaction. Subsequently, further characterization tests were carried out.

The chemical structures of scaffolds were investigated with FTIR analysis. According to results, the absorption peaks of beta sheet structures were identified in Amide I and II regions for SF:PLLA (1:3 w/w) and Amide I region for SF:PLLA (3:1 w/w) scaffolds. The methanol treatment seemed to result in beta sheet formation.

The water uptake analysis was applied on scaffolds for 1 and 24 hours. It was observed that increasing fibroin concentration in scaffolds resulted in higher water uptake capacities.

The degradation of scaffolds were investigated for two months. According to the results, the rate of degradation was similar between scaffolds until 6^{th} week but after 6 weeks, higher weight loss was observed while increasing fibroin concentration in scaffolds in the presence of protease enzyme.

Biomineralization process was carried out for 28 day. The weight changes of scaffolds incubated in 1x and 3xmSBF solutions were observed. The higher ion concentration of mSBF (3x) seemed to result in higher weight loss. The scaffolds incubated in 1xmSBF solution showed apparent weight gain whereas the less weight gain and weight loss at 3xmSBF samples. The effect of peptides could not be clearly observed from weight changes of samples.

The SEM images of scaffolds incubated in 1x and 3xmSBF solutions after 2, 3 and 4 week mineralization were investigated and EDS analysis were applied only to 1xmSBF samples because of the deformation of other scaffolds. According to the SEM images, the minerals were clearly observed on both scaffolds with and without peptides after 2^{nd} week of incubation but less mineralization (more calcification) appeared on few scaffolds after 3^{th} and 4^{th} week of incubation. According to the EDS results, a Ca/P atomic ratio closer to that of HAp were obtained in SF:PLLA (1:3 w/w) with peptides after 2^{th} week and SF:PLLA (3:1 w/w) with peptides after 4^{th} week mineralization. On the other hand, The more calcium accumulation were obtained in some samples that resulted in calcified surfaces especially after 3 and 4^{th} week mineralization in SF:PLLA (1:3 w/w) scaffolds with peptides.

The FTIR results showed the chemical structures of SF and PLLA polymers and also HAp granules on surfaces of scaffolds without peptides. According to the results, the characteristic absorption peaks of HAp crystals as OH^-, CO_3^{2-}, PO_4^{3-} were identified on spectra of both samples especially after 1^{st} week mineralization.

The proliferation of hFOB cells on composite scaffolds were investigated via MTS proliferation assay for 1, 4 and 7^{th} day. Briefly, the SF:PLLA (3:1 w/w) with and without peptide scaffolds showed higher cell attachment and proliferation than SF:PLLA (1:3 w/w) samples. The positive effect of peptides on cell proliferation was observed on SF:PLLA (1:3 w/w) samples but it seemed that peptides negatively affected cell proliferation for SF:PLLA (3:1 w/w) scaffolds.

For further prospects, the immobilization of peptides on surfaces can be investigated with HPLC to obtaine concentration of immobilized peptides. In addition, AFM surface characterization can be applied to observe the roughness of surfaces. The fluorescently labeled-peptides can be used to investigate the distribution of peptides on the surface. The *von Kossa stain (calcium stain)* can be applied on scaffolds to obtain the calcium deposition and distribution. Finally, scaffold composition and concentration of peptide can be optimized further to obtain ideal scaffolds.

REFERENCES

Al-Jallad, M., Atassi, Y., Mounif, E., Aressy, M., Tcharkhtchi, A. (2014). Oxidative solution polymerization of aniline hydrochloride onto electrospun nanofibers mats of polylactic acid: Preparation method and characterization, *Journal of Applied Polymer Science, **132***, p.41618 (1-7).

Altman, G. H., Horan, R. L., Lu, H. H., Moreau, J., Martin, I., Richmond, J. C., Kaplan, D.L. (2002). Silk matrix for tissue engineered anterior cruciate ligaments. *Biomaterials, **23***, 4131–41.

Andiappan, M., Sundaramoorthy, S., Panda, N., Meiyazhaban, G., Winfred, S. B., Venkataraman, G., Krishna, P. (2013). Electrospun eri silk fibroin scaffold coated with hydroxyapatite for bone tissue engineering applications. *Progress in Biomaterials, **2(6)***, 1-11.

Andrades, J. A., Claros, S., Jiménez-Palomo, P., López-Puertas, J. M., Zamora-Navas, P., Guerado, E., Monleón, M., Araque, M. C., Becerra, J. (2011). Skeletal Regeneration by Mesenchymal Stem Cells: What Else?. D. Eberli (Ed), *Regenerative Medicine and Tissue Engineering - Cells and Biomaterials* (ISBN 978-953-307-663-8). Retrieved from http://www.intechopen.com/books/regenerative-medicine-and-tissue-engineering-cells-and-biomaterials/skeletal-regeneration-by-mesenchymal-stem-cells-what-else-

Asefnejad, A., Behnamghader, A., Khorasani, M. T., Farsadzadeh, B. (2011). Polyurethane/fluor-hydroxyapatite nanocomposite scaffolds for bone tissue engineering. Part I: morphological, physical, and mechanical characterization. *International Journal of Nanomedicine, **6***, 93–100.

Barros, A. A., Aroso, I. M., Silva, T. H., Mano, J. F., Duarte, A. R. C., Reis, R. L. (2016). In vitro bioactivity studies of ceramic structures isolated from marine sponges, *Biomedical Materials, **11***, 1-11.

Barth, A. (2007). Infrared spectroscopy of proteins, *Biochimica et Biophysica Acta, **1767***, 1073–1101.

Birla, R. (2014). Introduction to Tissue Engineering: Applications and Challenges, Wiley-IEEE Press. doi: 10.1002/9781118886410.

Boccaccini, A. R., Gough, J. E. (2007). Tissue Engineering Using Ceramics and Polymers. Woodhead Publishing Series in Biomaterials.

Bunaciu, A. A., Fleschin, Ş. (2014). Aboul-Enein, H.Y. 2014. Evaluation of the Protein Secondary Structures Using Fourier Transform Infrared Spectroscopy, *Gazi University Journal of Science, **27(1)***, 637-644.

Ceyhan, T., Aşık, M., Atalar, A. C., Apohan, N. (2008). Menisküs yırtıklarının atroskopik tamirinde kullanılan poli L-laktik asit sabitleyicilerin erimeme nedenlerinin araştırılması, *Acta Orthop Traumatol Turc, **42(4)***, 284-288.

Cao, Y., Wang, B. (2009). Biodegradation of Silk Biomaterials, *International Journal of Molecular Sciences, **10***, 1514-1527.

Chae, J. C., Collier, J. P., Mayor, M. B., Suprenant, V. A., Dauphinais, L. A. (1992). Enhanced ingrowth of porous-coated cocr implants plasma-sprayed with ticalcium phosphate. *Journal of Biomedical Materials Research*, ***26***, 93-101.

Chang, P. C., Liu, B. Y., Liu, C. M., Chou, H. H., Ho, M. H., Liu, H. C., Wang, D. M., Hou, L.T. (2007). Bone tissue engineering with novel rhBMP2-PLLA composite scaffolds. *Journal of Biomedical Materials Research Part A,**81(4)***, 771-80.

Chavancy, G. (2005). Silkworm for non-textile industries. *Souveni, 20th congress of the international sericultural commission*, Bangalore, India, 15-18 December.

Chen, G., Ushida, T., Tateishi, T. (2002). Scaffold Design for Tissue Engineering. *Macromolecular Bioscience*, ***2***, 67-77.

Corin, K. A. and Gibson, L. J. (2010). Cell contraction forces in scaffolds with varying pore size and cell density. *Biomaterials, **31(18)***, 4835-45.

Dhert, W. J., Klein, C. P., Wolke, J. G., van der Velde, E. A., de Groot, K., Rozing, P. M. (1991). A mechanical investigation of fluorapatite, magnesiumwhitlockite, and hydroxylapatite plasma-sprayed coatings in goats. *Journal of Biomedical Materials Research, **25(10)***, 1183-200.

Do, A., Khorsand, B., Geary, S. M., Salem, A. K. (2015). 3D Printing of Scaffolds for Tissue Regeneration Applications. *Advanced Healthcare Materials, **4(12)***, 1742–1762.

Dopfer, O., Roth, D., Maier, J. P. (2002). Interaction of $C_3H_3^+$ isomers with molecular nitrogen:IR spectra of $C_3H_3^+$–$(N_2)_n$ clusters (n = 1–6), *International Journal of Mass Spectrometry*,***218***, 281–297.

Dubey, P., Murab, S., Karmakar, S., Chowdhury, P. K., Ghosh, S. (2015). Modulation of Self-Assembly Process of Fibroin: An Insight for Regulating the Conformation of Silk Biomaterials. *Biomacromolecules, **16*** **(12)**, 3936–3944.

Dzhoyashvili, N. A., Shen, S., Rochev, Y. A. (2015). Natural and Synthetic Materials for Self-Renewal, Long-Term Maintenance, and Differentiation of Induced Pluripotent Stem Cells. *Advanced Healthcare Materials, **4(16)***, 2342–2359.

Edwards, S. L., Mitchell, W., Matthews, J. B., Ingham, E., Russell, S.J. (2004). Design of Nonwoven Scaffold Structures for Tissue Engineering Of the Anterior Cruciate Ligament. *Autex Research Journal, **4(2)***, 86-94.

Epstein, N. E. (2011). Pros, cons, and costs of INFUSE in spinal surgery. *Surgical Neurology International, **2(10)***, doi: 10.4103/2152-7806.76147.

Eslahi, N., Hemmatinejad, N., Dadashian1, F. (2014). From Feather Waste to Valuable Nanoparticles, *Particulate Science and Technology, **32***, 242–250.

Fakirov, S. (2015). *Biodegradable Polyesters*, Weinheim Wiley-VCH.

Fang, L., Qi, R., Liu, L., Juan, G., Huang, S. (2009). Synthesis of Poly(L-lactide) via Solvothermal Method, International Journal of Polymer Science, 1-7. doi:10.1155/2009/929732

Figueiredo, M. M., Gamelas, J. A. F, Martins, A. G. (2012). Characterization of Bone and Bone-Based Graft Materials Using FTIR Spectroscopy, Prof. Theophanides Theophile (Ed), *Infrared Spectroscopy - Life and Biomedical Sciences*, InTech (pp. 315-339).

Fleet, M. E, Liu, X., King, P. L. (2004). Accommodation of the carbonate ion in apatite: An FTIR and X-ray structure study of crystals synthesized at 2–4 GPa, *American Mineralogist*, ***89***, 1422-1432.

Fortunati, E., Aluigi, A., Armentano, I., Morena, F., Emiliani, C., Martino, S., Santulli , C., Torre, L., Kenny, J. M., Puglia, D. (2015). Keratins extracted from Merino wool and Brown Alpaca fibres: Thermal,mechanical and biological properties of PLLA based biocomposites, *Materials Science and Engineering C*, ***47***, 394–406.

Ge, Y. P., Yuan, D., Luo, Z. L. Wang, B. B. (2014). Synthesis and characterization of poly(ester amide) from renewable resources through melt polycondensation, *eXPRESS Polymer Letters*, ***8(1)***, 50-54.

Georgieva, I., Mintcheva, N., Trendafilavo, N., Mitewa, M. (2001). IR study of the *N*, N^{I}, N^{II}- triphenylguanidine and its imine nitrogen coordinated Pd(II) complexes, *Vibrational Spectroscopy*, ***27***, 153-164.

Gerritsen, V.B. (2002). The tiptoe of an airbus. Protein Spotlight. Retrieved July, 2012. Available from http://web.expasy.org/spotlight/back_issues/024/

Gieseck, R. L., Hannan, N. R. F., Bort, R., Hanley, N. A., Drake, R. A. L., Cameron, G. W. W., Wynn, T. A., Vallier, L. (2014). Maturation of Induced Pluripotent Stem Cell Derived Hepatocytes by 3D-Culture. *PLoS ONE*, ***9(1)***, e86372. doi:10.1371/journal.pone.0086372

Gnecchi, M., Zhang, Z., Ni, A., Dzau, V. J. (2008). Paracrine mechanisms in adult stem cell signaling and therapy. *Circulation Research*, ***103(11)***, 1204-19. doi: 10.1161/CIRCRESAHA.108.176826.

Griffith, L. G. and Naughton, G. (2002). Tissue engineering-current challenges and expanding opportunities, *Science*, ***295(5557)***, 1009–1014.

Gulrajani, M. L. (1988). Degumming of silk; in Silk dyeing printing and finishing, Department of Textile Technology Indian Institute of Technology, New Delhi.

Hafeman, A. E., Li, B., Yoshii, T., Zienkiewicz, K., Davidson, J. M., Guelcher, S.A. (2008). Injectable biodegradable polyurethane scaffolds with release of platelet-derived growth factor for tissue repair and regeneration. *Pharmaceutical Research*, ***25(10)***, 2387-99.

Hanks, T. and Atkinson, B. L. (2004). Comparison of cell viability on anorganic bone matrix with or without P-15 cell binding peptide. *Biomaterials*, ***25(19)***, 4831-4836.

Hartgerink, J. D., Beniash, E., Stupp, S. I. (2001). Self-assembly and mineralization of peptide-amphiphile nanofibers. *Science*, ***294(5547)***, 1684–1688.

Hawari, A. A., Tham, C. Y., Hamid, Z. A. A. (2014). Effect of Synthesis Parameters on Size of the Biodegradable Poly (L-Lactide) (PLLA) Microspheres, *Advanced Materials Research*, ***858***, 60-66.

Ho, M., Hou, L. T., Tu, C. Y., Hsieh, H. J., Lai, J. Y., Chen, W. J., Wang, D. M. (2006). Promotion of cell affinity of porous PLLA scaffolds by immobilization of RGD peptides via plasma treatment. *Macromolecular Bioscience*, ***6(1)***, 90-8.

Hosseini, S., Naderi-Manesh, H., Mountassif, D., Cerruti, M., Vali, H., Faghihi, S. (2013). C-terminal Amidation of an Osteocalcin-Derived Peptide Promotes Hydroxyapatite Crystallization. *Journal of Biological Chemistry*, ***288(11)***, 7885-7893.

Hu, X., Kaplan, D., Cebe, P. (2006). Determining Beta-Sheet Crystallinity in Fibrous Proteins by Thermal Analysis and Infrared Spectroscopy, *Macromolecules, **39**,* 6161-6170.

Hu, X., Shmelev, K., Sun, L., Gil, E-S., Park, S-H., Cebe, P., Kaplan, D. L. (2011). Regulation of silk material structure by temperature-controlled water vapor annealing. *Biomacromolecules, **12(5)**,* 1686–1696.

Huang, J., Foo, C. W. P., Kaplan, D. L. (2007). Biosynthesis and applications of silk-like and collagenlike proteins. *Polymer Reviews, **47**,* 29-62.

Hutmacher, D. W. (2001). Scaffold design and fabrication technologies for engineering tissues--state of the art and future perspectives. *Journal of Biomaterials Science. Polymer, **12(1)**,* 107-24.

Innes, J. K., Ben-Nissan, B., Vago, B. (2002). Biomimetic conversion of Red Sea corraline structures for implant purposes, *Australasian Ceramic Society, **1**,* 21-22.

Itoh, D., Yoneda, S., Kuroda, S., Kondo, H., Umezawa, A., Ohya, K., Ohyama, T., Kasugai, S. (2002). Enhancement of osteogenesis on hydroxyapatite surface coated with synthetic peptide (EEEEEEEPRGDT) in vitro. *Journal of Biomedical Materials Research, **62(2)**,* 292-8.

Jeon, O., Song, S. J., Kang, S. W., Putnam, A. J., Kim, B. S. (2007). Enhancement of ectopic bone formation by bone morphogenetic protein-2 released from a heparin-conjugated poly(L-lactic-co-glycolic acid) scaffold. *Biomaterials, **28(17)**,* 2763–2771.

Jin, H. J., Kaplan, D. L. (2003). Mechanism of silk processing in insects and spiders. *Nature **424(6952)**,* 1057–1061.

Jin, H., Park, J., Karageorgiou, V., Kim, U., Valluzzi, R., Cebe, P., Kaplan, D. (2005). Water-stable silk films with reduced β -sheet content. *Advanced Functional Materials, **15(8)**,* 1241–1247.

Jones, G. L., Motta, A., Marshall, M. J., El Haj, A. J., Cartmell, S. H. (2009). Osteoblast: Osteoclast co-cultures on silk fibroin, chitosan and PLLA films. *Biomaterials, **30(29)**,* 5376-5384.

Jung, H. J., Ahn, K-D., Han, D. K. (2005). Surface Characteristics and Fibroblast Adhesion Behavior of RGD-Immobilized Biodegradable PLLA Films. *Macromolecular Research, **13(5)**,* 446-452.

Kaushiva, A., Turzhitsky, V. M., Darmoc, M., Backman, V., Ameer, G. A. (2007). A biodegradable vascularizing membrane: a feasibility study. *Acta Biomaterialia, **3(5)**,* 631–42.

Kim, H. J., Kim, U., Kim, H. S., Li, C., Wada, M., Leisk, G. G., Kaplan, D. L. (2008). Bone tissue engineering with premineralized silk scaffolds. *Bone, **42(6)**,* 1226-1234.

Kim, J., Magno, M. H. R., Waters, H., Doll, B. A., McBride, S., Alvarez, P., Darr, A., Vasanji, A., Kohn, J., Hollinger, J. O. (2012). Bone regeneration in a rabbit critical-sized calvarial model using tyrosine-derived polycarbonate scaffolds. *Tissue Engineering-Part A, **18**,* 1132–1139.

Kim, U. J., Park, J., Kim, H. J., Wada, M., Kaplan, D. L. (2005). Three-dimensional aqueous-derived biomaterial scaffolds from silk fibroin, *Biomaterials, **26**,* 2775-2785.

Kim, Y. S., Snively, C. M., Liu, Y., Rabolt, J. F., Chase, D. B. (2008). Real-Time Imaging of Crystallization in Polylactide Enantiomeric Monolayers at the Air-Water Interface. *Langmuir*, ***24***, 10791-10796.

Krikorian, V., Pochan, D. J. (2005). Crystallization Behavior of Poly(L-lactic acid) Nanocomposites: Nucleation and Growth Probed by Infrared Spectroscopy. *Macromolecules*, ***38***, 6520-6527.

Kundu, B., Kurland, N. E., Bano, S., Patra, C., Engel, F. B., Yadavalli, V. K., Kundu, S. C. (2014). Silk proteins for biomedical applications: Bioengineering perspectives, *Progress in Polymer Science, **39(2)***, 251-267.

Langer, R. and Tirrell, D. A. (2004). Designing materials for biology and medicine. *Nature*, ***428***, 487–492.

Langer, R. and Vacanti, J. (1993). Tissue engineering. *Science, **260(5110)***, 920–926.

Lee, J. Y., Chooa, J. E., Choia, Y.S., Park, J. B., Mind, D.S., Lee, S. J., Rhyuf, H. K., Jog, I. H., Chungb, J. P., Park, Y. J. (2007). Assembly of collagen-binding peptide with collagen as a bioactive scaffold for osteogenesis in vitro and in vivo. *Biomaterials, **28(29)*, 4257-4267**

Li, M., Ogiso, M. (2003). Minoura, N. Enzymatic degradation behavior of porous silk fibroin sheets. *Biomaterials*, ***24***, 357-365.

Li, W. J., Cooper, JA Jr., Mauck, R. L., Tuan, R. S. (2006). Fabrication and characterization of six electrospun poly(alpha-hydroxy ester)-based fibrous scaffolds for tissue engineering applications. *Acta Biomaterialia*, ***2(4)***, 377–85.

Li, W. J., Laurencin, C. T., Caterson, E. J., Tuan, R. S., Ko, F. K. (2002). Electrospun nanofibrous structure: A novel scaffold for tissue engineering. *Journal of Biomedical Materials Research*, ***60(4)***, 613-621.

Liang, **W-H., Kienitz**, **B. L., Penick**, **K. J., Welter**, **J. F., Zawodzinski**, **T. A., Baskaran**, **H**. (2010). Concentrated Collagen-Chondroitin Sulfate Scaffolds for Tissue Engineering Applications, *Journal of Biomedical Materials Research A*, ***94(4)***, 1050-1060.

Liu, H. (2016). *Nanocomposites for Musculoskeletal Tissue Regeneration. Woodhead Publishing*. California: Woodhead Publishing.

Liu, X. And Ma, P. X. (2004). Polymeric Scaffolds for Bone Tissue Engineering. *Annals of Biomedical Engineering*, ***32(3)***, 477-486.

Lo, H., Kadiyala, S., Guggino, S. E., Leong, K. W. (1996). Poly(L-lactic acid) foams with cell seeding and controlled-release capacity. *Journal of Biomedical Materials Research*, ***30(4)***, 475-84.

Lu, T., Li, Y., Chen, T. (2013). Techniques for fabrication and construction of three-dimensional scaffolds for tissue engineering. *International Journal of Nanomedicine*, ***8***, 337-350.

Lu, L., Peter, S. J., Lyman, M. D., Lai, H-L., Leite, S. M., Tamada, J. A., Uyama, S., Vacanti, J. P., Langer, R., Mikos, A. G. (2000). In vitro and in vivo degradation of porous poly (dl-lactic-co-glycolic acid) foams. *Biomaterials*, ***21***, 1837–45.

Lu, Q., Wang, X., Zhu, H., Kaplan, D. L. (2011). Surface Immobilization of antibody on silk fibroin through conformational transition, *Acta Biomateria, **7(7)***, 2782-2786.

Mandal, B. B. and Kundu, S. C. (2009). Cell proliferation and migration in silk fibroin 3D scaffolds. *Biomaterials,* ***30(15)***, 2956-2965.

Martin, C., Winet, H., Bao, J. Y. (1996). Acidity near eroding polylactidepolyglycolide in vitro and in vivo in rabbit tibial born chambers. *Biomaterials,* ***17***, 2373–2380.

Middleton, J. C., Tipton, A. J. (2000). Synthetic biodegradable polymers as orthopedic devices. *Biomaterials,* ***21(23)***, 2335–46.

Mohanty, S., Nayak, S. K., Kaith, B. S., Kalia, S. (2015). *Polymer Nanocomposites based on Inorganic and Organic Nanomaterials*, Scrivener Publishing: Massachusetts.

Mondal, M., Trivedy, K., Kumar, S. N. (2007). The silk proteins, sericin and fibroin in silkworm, Bombyx mori Linn., - a review. *Caspian Journal of Environmental Sciences,* ***5(2)***, 63-76.

Monti, P., Freddi, G., Arosio, C., Tsukada, M., Arai, T., Taddedi, P. (2007). Vibrational spectroscopic study of sulphated silk proteins, *Journal of Molecular Structure,* ***834–836*** , 202–206.

Nazarov, R., Jin, H. J., Kaplan, D. L. (2004). Porous 3-D Scaffolds from Regenerated Silk Fibroin. *Biomacromolecules,* ***5(3)***, 718-726.

Nerem, R. M. and Sambanis, A. (1995). Tissue engineering: from biology to biological substitutes. *Tissue Engineering. Spring,* ***1(1)***, 3-13. doi: 10.1089/ten.1995.1.3.

Neuman, W. F. and Neuman, M. W. (1958). *The chemical dynamics of bone mineral.* Chicago: The University of Chicago Press.

Nogueira1, T., Gonçalves, N., Botan, R., Wypych, F., Lona1, L. (2016). Layered double hydroxides as fillers in poly(l-lactide) nanocomposites, obtained by in situ bulk polymerization, *Polímeros,* ***26(2)***, 106-114.

Orue, A., Eceiza, A., Peña-Rodriguez, C., Arbelaiz, A. (2016). Water Uptake Behavior and Young Modulus Prediction of Composites Based on Treated Sisal Fibers and Poly(Lactic Acid), *Materials,* ***9***, 400, doi:10.3390/ma9050400.

Palmer, L. C., Newcomb, C. J., Kaltz, S. R., Spoerke, E. D., Stupp, S. I. (2008). Biomimetic Systems for Hydroxyapatite Mineralization Inspired By Bone and Enamel. *Chemical Reviews,* ***108(11),*** 4754-4783.

Pan, H., Zheng, Q., Yang, S., Guo, X. (2014). Effects of functionalization of PLGA-[Asp-PEG]n copolymer surfaces with Arg-Gly-Asp peptides, hydroxyapatite nanoparticles, and BMP-2-derived peptides on cell behavior in vitro. *Journal of Biomedical Materials Research,* ***102(12)***, 4526-35.

Park, J. B. (1984). *Biomaterials Science and Engineering*. New York: Plenum Press.

Patel, H., Bonde, M., Srinivasan, G. (2011). Biodegradable Polymer Scaffold for Tissue Engineering. *Trends in Biomaterials & Artificial Organs,* ***25(1)***, 20-29.

Prabu S, l., TNK, Suriyaprakash, K., Rckmani, R., Thirumurugan. (2014). Preparation and Characterization of Biodegradable Glimepiride Loaded PLA Nanoparticles by o/w Solvent Evaporation Method Using High Pressure Homogenizer: A Factorial Design Approach, *SAJ Pharmacy and Pharmacology,* ***1(1)***, 1-10.

Qiang, L. and Zhang, H. (2010).Controlled freezing and freeze drying: a versatile route for porous and micro-/nano-structured materials. *Journal of Chemical Technology and Biotechnology,* ***86***, 172-184.

Qiao, C., Zhang, K., Jin, H., Miao, L., Shi, C., Liu, X., Yuan, A., Liu, J., Li, D., Zheng, C., Zhang, G., Li, X., Yang, B., Sun, H. (2013). Using poly(lactic-co-glycolic acid) microspheres to encapsulate plasmid of bone morphogenetic protein 2/polyethylenimine nanoparticles to promote bone formation in vitro and in vivo. *International Journal of Nanomedicine, **8***, 2985–2995.

Radev, L, Gerganov, T., Georgiev, H., Kolev, A., Vassileva, V., Iankova, R., Cholakova, E. (2013). Silk Fibroin/Calcium Phosphate Silicate Composites: In vitro Bioactivity. *International Journal of Materials and Chemistry, **3(3A)***, 8-15. doi: 10.5923/s.ijmc.201303.02.

Ren, F., Lu, X., Leng, Y. (2013). Ab initio simulation on the crystal structure and elastic properties of carbonated apatite. *Journal of the Mechanical Behavior of Biomedical Materials, **26***, 59-67.

Rockwood, D. N., Preda, R. C., Yücel, T., Wang, X., Lovett, M. L., Kaplan, D. L. (2011). Materials Fabrication from Bombyx mori Silk Fibroin. *Nature Protocols, **6(10),*** doi:10.1038/nprot.2011.379.

Roy, M. D., Stanley, S. K., Amis, E. J., Becker, M. L. (2008). Identification of a Highly Specific Hydroxyapatite-binding Peptide using Phage Display, *Advanced Materials, **20(10)***, 1830-1836.

Saito, E., Liao, E. E., Hu, W., Krebsbach, P. H., Hollister, S. J. (2013). Effects of designed PLLA and 50:50 PLGA scaffold architectures on bone formation in vivo. *Journal of Tissue Engineering and Regenerative Medicine, **7(2)***, 99-111.

Sallam, S. M., Tohami, K. M., Sallam, A. M., Abo Salem, L. I., Mohamed, F.A. (2012). The influence of chromium ions on the growth of the calcium hydroxyapatite crystal, *Journal of Biophysical Chemistry, **3(4)***, 283-286.

Schulte, J. (2004). Proceedings of the Asia Pacific Nanotechnology Forum 2003 : OZ Nano 03, World Scientific.: River Edge, NJ.

Shalaby, S. W., Burg, K. J. L. (2003). *Absorbable and Biodegradable Polymers*. Boca Raton: CRC press.

Sharma, B. K. (2000). *Instrumental Methods of Chemical Analysis*,GOEL Publishing House: Meerut.

Shastri, V.P., Martin, R., Langer, R. (2000). Microporous polymer foams by hydrocarbon templating in. *Proceeding of the National Academy of Sciences USA, **97(5)***, 1970-1975.

Shi, Y., Hu, D., Xin, Z., Zhao, S., Zhou, S., Meng, X. (2016). Conformation order of poly(L-lactic acid) chains during the melt crystallization process: infrared and two-dimensional infrared correlation spectroscopy study, *Journal of Materials Science, **51***, 4880-4887.

Shi, P., Teh, T. K. H., Toh, S. L., Goh, J. C. H. (2013). Variation of the effect of calcium phosphate enhancement of implanted silk fibroin ligament bone integration. *Biomaterials, **34***, 5947-5957.

Shimura, K., Kikuchi, A., Katagata, Y., Ohotomo, K. (1982). The Occurrence of Small Component Proteins in the Cocoon Fibroin of *Bombyx mori*. *The Journal of Sericultural Science of Japan, **51(1)***, 20 -26.

Shrivats, A. R., McDermott, M. C., Hollinger, J. O. (2014). Bone tissue engineering: state of the Union. *Drug Discovery Today, **19(6)***, 781-6. doi: 10.1016/j.drudis.2014.04.010.

Sobczak, M., Witkowska, E., Olędzka, E., Kolodziejski, W. (2008). Synthesis and Structural Analysis of Polyester Prodrugs of Norfloxacin, *Molecules*, ***13***, 96-106.

Spevak, L., Flach, C. R., Hunter, T., Mendelsohn, R., Boskey, A. (2013). FTIRI Parameters describing Acid Phosphate Substitution in Biologic Hydroxyapatite, *Calcified Tissue International*, ***92(5)***, 418-428.

Sung, H-J, Meredith, C., Johnson, C., Galis, Z. S. (2004). The effect of scaffold degradation rate on three-dimensional cell growth and angiogenesis. *Biomaterials*, ***25***, 5735-5742.

Tanaka, K., Inoue, S., Mizuno, S. (1999). Hydrophobic interaction of P25, containing Asn-linked oligosaccharide chains, with the H-L complex of silk fibroin produced by Bombyx mori. *Insect Biochemistry and Molecular Biology*, ***29(3)***, 269-276.

Tho, N. T. M., An, T. N. M., Tri, M. D., Sreekanth, T. V. M., Lee, J., Nagajyothi, P.C., Lee, K. D. (2013). Green Synthesis of Silver Nanoparticles Using Nelumbo *nucifera* Seed Extract and its Antibacterial Activity, *Acta Chimica Slovenica*, ***60***, 673-678.

Tunma1, S., Kanjai, E., Nuandee1, J., Boonyawan, D. (2013). Immobilization of Silk Fibroin as Scaffold for Cell Culture by Plasma Grafting Polymerization, *Advanced Materials Research*, ***802***, 53-58.

Ulman, A. (1991). An Introduction To Ultrathin Organic Films: From Langmuirblodgett To Self-Assembly; Academic press: San Diego.

Valluzzi, R. and Gido, S. P. (1997). The crystal structure of Bombyx mori silk fibroin at the air–water interface. *Biopolymers*, ***42(4)***, 705-717.

Venkatasubbu, C. D., Ramasamy, S., Ramakrishnan, V., Avadhani, G. S., Thangavel, **R., Kumar, J.** (2011). Investigations on Zinc Doped Nanocrystalline Hydroxyapatite, *International Journal of NanoScience and Nanotechnology*, ***2(1)***, 1-23.

Wan, Y., Fang, Y., Wu, H., Cao, X. (2007). Porous polylactide/chitosan scaffolds for tissue engineering. *Journal of Biomedical Materials Research Part A*,***80(4)***, 776-89.

Wojasinski, M., Faliszewski, K., Ciach, T. (2013). *Electrospinning Production of PLLA Fibrous Scaffolds for Tissue Engineering.* Warsaw University of Technology, Faculty of Chemical and Process Engineering, POLAND.

Yang, S. F., Leong, K. F., Du, Z. H., Chu, C. K. (2002). The design of scaffolds for use in tissue engineering Part II. Rapid prototyping techniques. *Tissue Engineering*, ***8***, 1–11.

Z**hang, R., Ma, P. X.** (2004) Biomimetic polymer/apatite composite scaffolds for mineralized tissue engineering. *Macromolecular Bioscience*, ***4(2)***, 100–11.

Zhang, R., Ma, P. X. (1999). Porous poly(ι-lactic acid)/apatite composites created by biomimetic process. *Journal of Biomedical Materials Research*, ***45(4)***, 285-93.

Zhang, R. and Ma., P. X. (2001). Processing of polymer scaffolds: Phase separation. In A. Atala, R. Lanza (Eds), *Methods of Tissue Engineering* (pp. 715–724). San Diego, CA: Academic Press.

Zhang, K., Wang, H., Huang, C., Su, Y., Mo, X., Ikada, Y. (2010). Fabrication of silk fibroin blended P(LLA-CL) nanofibrous scaffolds for tissue

engineering. *Journal of Biomedical Materials Research Part A,**93(3)***, 984-93.

Zimmermann, M., Brambilla, V., Brandalise, R.N., Zattera, A.J. (2013). Observations of the Effects of Different Chemical Blowing Agents on the Degradation of Poly(Lactic Acid) Foams in Simulated Soil, *Materials Research, **16(6)***, 1266-1273. doi: 10.1590/S1516-14392013005000133

APPENDICES

APPENDIX A: Chemicals and Materials

APPENDIX B: Preparation of 1x Phosphate Buffered Saline (PBS) Buffer

APPENDIX C: Preparation of 1x and 3x Modified Simulated Body Fluid (mSBF) Buffer

APPENDIX D: Laboratory Equipment

APPENDIX A

Chemical/Material	Supplier
Poly (L-Lactic Acid), PLLA	Sigma-Aldrich
Bombyx Mori cocoons	Bursa Kozabirlik
Methanol, CH_3OH	Sigma-Aldrich
Ethanol, C_2H_6O	Sigma-Aldrich
Lithium bromide, LiBr	Sigma-Aldrich
Hexafluoroisopropanol, HFIP	Sigma-Aldrich
1-ethyl-3-(3-dimethylaminopropyl)carbodiimide, EDC	Sigma-Aldrich
N-hydroxysuccinimide, NHS	Sigma-Aldrich
Sodium azide, NaN_3	Merck Millipore
Sodium chloride, NaCl	Merck Millipore
Potassium chloride, KCl	Sigma-Aldrich
Sodium phosphate dibasic, Na_2HPO_4	Sigma-Aldrich
Potassium phosphate monobasic,KH_2PO_4	Sigma-Aldrich
2-(N-morpholino)ethanesulfonic acid, MES	Sigma-Aldrich
Di-potassium hydrogen phosphate trihydrate, $HK_2O_4P.3H_2O$	Sigma-Aldrich
4-(2-hydroxyethyl)-1-piperazineethanesulfonic acid, HEPES	Biomatik
Magnesium chloride hexahydrate, $Cl_2Mg.6H_2O$	Sigma-Aldrich
Sodium sulphate, Na_2SO_4	Sigma-Aldrich
Sodium bicarbonate, $CHNaO_3$	Sigma-Aldrich
Calcium chloride, $CaCl_2$	Sigma-Aldrich
Sodium carbonate, Na_2CO_3	Sigma-Aldrich
Hydrochloride, HCl	Sigma-Aldrich
Sodium hydroxide, NaOH	Sigma-Aldrich
Protease XIV	Sigma-Aldrich
Dulbecco's Modified Eagle Medium, DMEM	Sigma-Aldrich
Penicillin Streptomycin Solution	Sigma-Aldrich
Fetal Bovine Serum	Sigma-Aldrich
Trypan Blue 0.4%	Sigma-Aldrich
MTS Cell Proliferation Colorimetric Assay Kit	Sigma-Aldrich

APPENDIX B

1. The following materials were weighed in the amount mentioned below and dissolved in 800 mL ultrapure water:
    - 8 g of sodium chloride (NaCl)
    - 0.2 g of potassium chloride (KCl)
    - 1.44 g of sodium phosphate dibasic (Na_2HPO_4)
    - 0.24 g of potassium phosphate monobasic (KH_2PO_4)
2. The pH of the solution was adjusted to 7.4 with hydrochloride (HCl).
3. The total volume of the solution was adjusted to 1 litre with ultrapure water.
4. The solution was filtrated by 0.45 μm filter.

APPENDIX C

1. All apparatus to be used for preparation of mSBF solution were washed with 1.0 M of HCl and ultrapure water.
2. 700 mL of ultrapure water were poured into a 1 litre polypropylene beaker that was stirred using a magnetic bar at room temperature.
3. The reagents listed below were added according to the order and amounts given in the list and completely dissolved. The HEPES was previously dissolved in 100 mL of aqueous 0.2 M NaOH.
   NaCl: 5.403 g
   $NaHCO_3$: 0.504 g
   Na_2CO_3: 0.426 g
   KCl: 0.225 g
   K_2HPO_4.3H2O: 0.230 g
   $MgCl_2$.6H2O: 0.311 g
   HEPES: 17.892 g
   $CaCl_2$: 0.293 g
   Na_2SO_4: 0.072 g
   NaOH (1.0 M): 15 mL
4. The fluid was adjusted to a final pH of 7.4 at room temperature by titrating aqueous 1.0 M of NaOH into the fluid.
5. The total volume of the fluid was adjusted to 1 litre by adding ultrapure water.
6. The freshly prepared mSBF solution was sterilized by using 0.22 μm pore size filters.
7. The solution was stored at 37 ^{o}C in polypropylene falcons during biomineralization process.

In order to prepare a 3x mSBF solution, the amounts of the ingredients above were multiplied by 3. All remaining steps were applied in the same way.

APPENDIX D

Equipment	Supplier
Refrigerator, +4 ^{o}C	Vestel
Magnetic stirrer	Cole-Parmer
Scale	Precisa Gravimetrics AG
Freezer, -20 ^{o}C	Arçelik
Freeze-dryer	Martin Christ
pH metre	WTW GmbH
Rocking platform shaker	Heidolph Instruments
Heating/Drying oven	Memmert GmbH + Co. KG
Centrifuge	Beckman Coulter
Pipettes	Eppendorf
Beakers	ISOLAB
Tissue culture test plates	TPP Techno Plastic Products AG
Scanning electron microscope, SEM	FEI Quanta 600
Energy-dispersive X-ray spectroscopy	FEI
Mini Sputter Coater	SC7620 Polaron Ranger
Dialysis cassettes	Thermo Scientific
Syringe and needle	BD Medical
Ultrapure water system	TKA-Pacific
Fourier transform infrared spectroscopy, FTIR	Perkin Elmer

CURRICULUM VITAE

Name Surname **:** İnas ÖZCAN

Place and Date of Birth **:** Arabistan, 20 November 1991

E-Mail **:** ins.ozcn@gmail.com

EDUCATION

- **B.Sc.** **:** 2013, Yıldız Technical University, Faculty of Chemical and Metallurgical Engineering, Department of Bioengineering

PROFESSIONAL EXPERIENCE AND REWARDS:

- Part-time Intern, Abdi İbrahim İlaç San.ve Tic. A.Ş. (March 2016, Present)
- Intern, Anadolu Efes Biracılık ve Malt Sanayii A.Ş. (January 2013-February 2013)
- Intern, T.C. Adalet Bakanlığı Adli Tıp Kurumu (August 2011-September 2011)